Journal Pre-proof

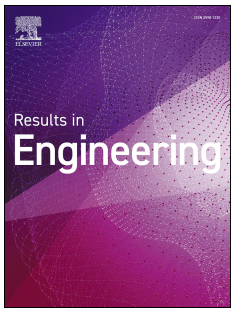

Stability Analysis for the Phytoplankton-Zooplankton Model with Depletion of Dissolved Oxygen and Strong Allee Effects

Ahmed Ali, Shireen Jawad, Ali Hasan Ali, Matthias Winter

PII: S2590-1230(24)00444-4

DOI: https://doi.org/10.1016/j.rineng.2024.102190

Reference: RINENG 102190

To appear in: *Results in Engineering*

Received Date: 29 October 2023

Revised Date: 20 April 2024

Accepted Date: 26 April 2024

Please cite this article as: A. Ali, S. Jawad, A.H. Ali, M. Winter, Stability Analysis for the Phytoplankton-Zooplankton Model with Depletion of Dissolved Oxygen and Strong Allee Effects, *Results in Engineering*, https://doi.org/10.1016/j.rineng.2024.102190.

Stability Analysis for the Phytoplankton-Zooplankton Model with Depletion of Dissolved Oxygen and Strong Allee Effects

Ahmed Ali [1], Shireen Jawad [1] Ali Hasan Ali [2,*], Matthias Winter [3]

[1] Department of Mathematics, College of Science, University of Baghdad, Baghdad 10071, Iraq; (A.A: ahmedali.970q6@gmail.com), (S.J: shireen.jawad@sc.uobaghdad.edu.iq).
[2] Institute of Mathematics, University of Debrecen, Pf. 400, H-4002 Debrecen, Hungary; (A.H.A: ali.hasan@science.unideb.hu)
[3] Department of Mathematics, Brunel University London, Uxbridge UB8 3PH, UK; (M.W: matthias.winter@brunel.ac.uk)
* Correspondence: ali.hasan@science.unideb.hu

Abstract

The photosynthetic activity of phytoplankton in the seas is responsible for an estimated 50-80% of the world's oxygen generation. Both phytoplankton and zooplankton require some of this synthesized oxygen for cellular respiration. This study aims to better understand how the oxygen-phytoplankton dynamics are altered due to the Allee effect in phytoplankton development, particularly when considering the time-dependent oxygen generation rate. The dynamic analysis of the model is dedicated to finding the possible equilibrium points. The analysis reveals that three equilibrium points can be obtained. The stability study demonstrates that one of the equilibrium points is always stable. The remaining equilibrium points are stable under specific conditions. We also identify bifurcations originating from these equilibrium points, including transcritical, pitchfork, and Hopf bifurcation. We derive conditions for stable limit cycles (supercritical Hopf bifurcation) and, in some cases, establish the non-existence of solutions. Numerical simulations are performed to validate our theoretical findings. Furthermore, it is noted that the Allee threshold for the phytoplankton population (k_0) significantly influences the overall dynamics of the system. When $k_0 \leq 0.001$, the population of plankton is at risk of extinction. On the other hand, when $0.001 < k_0 \leq 0.01$, the population of zooplankton is at risk of extinction. When $0.01 < k_0 \leq 2$, the solution reaches a stable condition of coexistence. Conversely, when $k_0 \geq 2.1$, the solution exhibits periodic attractor behavior.

***Key-words*:** Plankton interaction; Strong Allee effect; Dissolved Oxygen; Stability analysis; Hopf bifurcation.

***MSC 2020*:** 34D05, 34D20, 34D23, 34D45, 92D40, 92D25.

1. Introduction

Understanding dissolved oxygen dynamics has received much interest because it is such a key indicator for the health of the marine ecosystem [1]–[3]. Phytoplankton, the planktonic communities most resembling plants, supply the vast majority of the oxygen in the oceans through photosynthesis and serve as the foundation of the marine food chain. It is commonly known that the amount of oxygen generated by phytoplankton varies significantly due to environmental fluctuations such as the rate of salinity, the level of temperature, and the number of nutrients. Further, phytoplankton's oxygen production varies dramatically throughout the day and night. Therefore, the link between phytoplankton and dissolved oxygen is essential to the survival of most species, from the simplest (a single cell) to the most sophisticated (a human being). Changes in oxygen production can have profound consequences for marine life [4]. For instance, some environmental factors, including temperature, affect phytoplankton's biomass and growth. Dissolved oxygen levels in water fluctuate on a daily cycle since oxygen is created during photosynthesis (during the day) and absorbed during respiration (at all times). Phytoplankton communities are, therefore, valuable indicators of environmental changes [5]–[8]. For example, Mondal, Samanta and De la Sen have investigated how the coupled plankton-oxygen dynamics in the ocean is affected by a low oxygen production rate which can lead to oxygen depletion and plankton extinction [9].

Most modelers generally select the Logistic growth form as the growth function for the prey species without considering the predator species [10]–[12]. However, it is common knowledge that the resources available in an ecosystem, such as space, food, and the components of essential nutrition, are finite. As the population grows, the average growth rate steadily decreases. The average growth rate drops to zero as the population meets the environment's carrying capacity, k, and drops further for any population size greater than k. Further, a substantial body of research suggests that a low population density actually has the opposite effect. The Allee effect is the name of this phenomenon, which describes the positive density dependency of population increase in areas with low densities [13].

On the other hand, the study of theoretical ecology has as its primary goal the identification of the various dynamical mechanisms linked with interactions between prey and predator [14]–[16]. An example of a particular type of predator-prey interaction that opens up various facets of marine ecology is the relationship between phytoplankton and zooplankton. Phytoplankton significantly contributes to aquatic ecosystems, including producing an enormous amount of oxygen, managing natural resources and water quality, and providing the basis for various food webs [17]–[18]. Research on the dynamics of plankton is a fascinating topic. The building blocks of all aquatic food chains can be found in plankton, with phytoplankton occupying the first trophic level of the food chain [19]. Phytoplankton toxins play a critical environmental function and can not be disregarded. Environmental stress factors, optimal environmental circumstances, nutrient-limited settings, and other similar characteristics are significant contributors to the release of toxins. Some phytoplankton species are notorious for producing and releasing toxic or allelochemicals into the environment, which can be detrimental to other plankton species [20]. For instance, Venturino,

Chattopadhyay and their colleagues have demonstrated that toxin-producing phytoplankton works as a controlling agent for the cessation of plankton blooms [21]. Dhar and Baghel consider the effect of dissolved oxygen on the presence of an interacting planktonic population. They conclude that the possibility of Hopf-bifurcation in the interior equilibrium could occur if the phytoplankton growth rate is chosen as the bifurcation parameter [22].

The objective of this research is to investigate the dynamics of the oxygen-plankton model as a result of the combined influence of the Allee effect on the growth of phytoplankton and the time-dependent oxygen production rate in particular. Considering these effects, we propose a DOPZ model of dissolved oxygen- phytoplankton- zooplankton interaction with a strong Allee effect on phytoplankton growth. This paper's findings provide additional context for [22] by

- Replacing the linear form in the growth rate of the phytoplankton population with growth in the form of the strong Allee effect.
- In addition, our model includes both toxic and non-toxic phytoplankton, and we assume the zooplankton consumes both.
- Further, we consider that some phytoplankton species have a low chance of being eaten by zooplankton by hiding in the various sediments on the seafloor. These sediments provide the prey with a place to hide from their predators.
- Finally, since the phytoplankton performs photosynthesis throughout the day, they release oxygen into the atmosphere. this phenomenon has been considered in our model.

After presenting the construction of our model, then our goal is to observe the impact of the Allee threshold on the dynamics of a DOPZ model. In addition, the comprehension of the nonlinear dynamics of our model will be discussed by employing different methodologies such as stability and bifurcation analysis techniques. Finally, we will verify the accuracy of our analytical results by simulating the proposed system numerically.

2. Construction of the Model

Our work involves a 3D model of an aquatic system with three components: phytoplankton $u(t)$, zooplankton $v(t)$, and concentration of dissolved oxygen $w(t)$. The following presumptions form the basis of the mathematical model that will aid in our understanding of the dynamics of the DOPZ system.

The phytoplankton population is assumed to come in two types, toxic and non-toxic which can occasionally release harmful substances [23]. phytoplankton species are assumed to grow according to the strong Allee effect type of growth. The term $\frac{ru}{(a_1+w_0-w)}\left(1-\frac{u}{k}\right)\left(\frac{u}{k_0}-1\right)$ stands for the Allee effect type growth of phytoplankton, combining the absorption of dissolved oxygen with the growth rate r, the maximal phytoplankton carrying capacity k and the critical phytoplankton level k_0 (Allee threshold) such that $0 < k_0 < k$ [11]. When the population density drops below the critical threshold k_0, the population starts to decrease, and the population tends to extinction. w_0 is the constant concentration of dissolved oxygen that comes from several sources

in the water; a_1 is the phytoplankton saturation constant; δ_1 denotes the phytoplankton's natural death rate; $\alpha_1 u(1-m)v$ represents the predation of the available phytoplankton by zooplankton. In addition, we consider that some phytoplankton populations have a low chance of being eaten by zooplankton by hiding in the various sediments that may be found on the seafloor. These sediments provide the prey with a place to hide from their predators [24]. Hence, $(1-m)$ represents the proportion of unprotected phytoplankton consumed by various zooplankton types. Thus the phytoplankton equation has the following form:

$$\frac{du}{dt} = \frac{ru}{(a_1+w_0-w)}\left(1-\frac{u}{k}\right)\left(\frac{u}{k_0}-1\right) - \alpha_1 u(1-m)v - \delta_1 u.$$

It is assumed that zooplankton feeds on the two categories mentioned above according to a modified Holling type I and II response [22], [25]. Thus, $\frac{\alpha_2 u(1-m)v}{(a_2+w_0-w)}$ denotes the conversion from phytoplankton to zooplankton; a_2 is the zooplankton saturation constant; $au(1-m)v$ stands for the predation of toxic phytoplankton by zooplankton; δ_2 represents the zooplankton's natural death rate. Therfore, the equation of zooplankton species can be written as

$$\frac{dv}{dt} = \frac{\alpha_2 u(1-m)v}{(a_2+w_0-w)} - \delta_2 v - au(1-m)v$$

$w(t)$ represents the oxygen concentration in an aquatic environment. Further, since the phytoplankton performs photosynthesis throughout the day, they release oxygen into the atmosphere. Additionally, the rate of oxygen depletion can be attributed to various factors, including the consumption of oxygen by phytoplankton during the night, the respiration of marine animals, and the gradual decline in oxygen concentration that results from chemical reactions that take place in the water [26]. Thus, $s(w_0-w)$ represents the dissolved oxygen concentration that comes from other sources, du represents the amount of oxygen produced as a result of the process of photosynthesis carried out by phytoplankton. $\gamma_1 uw$ is the consumption of oxygen by phytoplankton during the night. $\gamma_2 vw$ denotes the consumption of oxygen by zooplankton. γ is the natural depletion rate of oxygen. In this case, the dissolved oxygen equation can be written as:

$$\frac{dw}{dt} = s(w_0-w) + du - \gamma w - \gamma_1 uw - \gamma_2 vw.$$

The following set of ordinary differential equations serves as the governing structure for the dynamical system of the DOPZ model:

$$\begin{aligned}
\frac{du}{dt} &= \frac{ru}{(a_1+w_0-w)}\left(1-\frac{u}{k}\right)\left(\frac{u}{k_0}-1\right) - \alpha_1 u(1-m)v - \delta_1 u = f_1(u,v,w),\\
\frac{dv}{dt} &= \frac{\alpha_2 u(1-m)v}{(a_2+w_0-w)} - \delta_2 v - au(1-m)v = f_2(u,v,w),\\
\frac{dw}{dt} &= s(w_0-w) + du - \gamma w - \gamma_1 uw - \gamma_2 vw = f_3(u,v,w),
\end{aligned} \tag{1}$$

with the initial conditions $u(0) = u_{00} \geq 0, v(0) = v_{00} \geq 0$. All parameters for the dissolved oxygen-phytoplankton-zooplankton model (DOPZ) are expected to be positive and clarified in Table 1.

Table 1. The biological interpretation of the DOPZ system's parameters.

Parameters	**Biological interpretation**
$\boldsymbol{r}$	The growth rate of phytoplankton.
$\boldsymbol{\alpha_1}$	The capture rate of the available non-toxic phytoplankton by zooplankton.
$\boldsymbol{m} \in (\boldsymbol{0}, \boldsymbol{1})$	The proportion of protected phytoplankton.
$\boldsymbol{\alpha_2}$	The conversion rate from phytoplankton to zooplankton.
$\boldsymbol{a}$	The predation rate of toxic phytoplankton by zooplankton.
$\boldsymbol{\delta_1}$	The phytoplankton's natural death rate.
$\boldsymbol{\delta_2}$	The zooplankton's natural death rate.
$\boldsymbol{a_1}$	The phytoplankton saturation constant.
$\boldsymbol{a_2}$	The zooplankton saturation constant.
$\boldsymbol{w_0}$	The constant concentration of dissolved oxygen that comes from other sources.
$\boldsymbol{s}$	The replenishment rate of oxygen in the marine.
$\boldsymbol{d}$	The amount of oxygen produced as a result of the process of photosynthesis carried out by phytoplankton.
$\boldsymbol{\gamma}$	The natural depletion rate of oxygen.
$\boldsymbol{\gamma_1}$	The consumption of oxygen by phytoplankton during the night.
$\boldsymbol{\gamma_2}$	The consumption of oxygen by zooplankton.

Further, Figure 1 illustrates the schematic sketch of the DOPZ model.

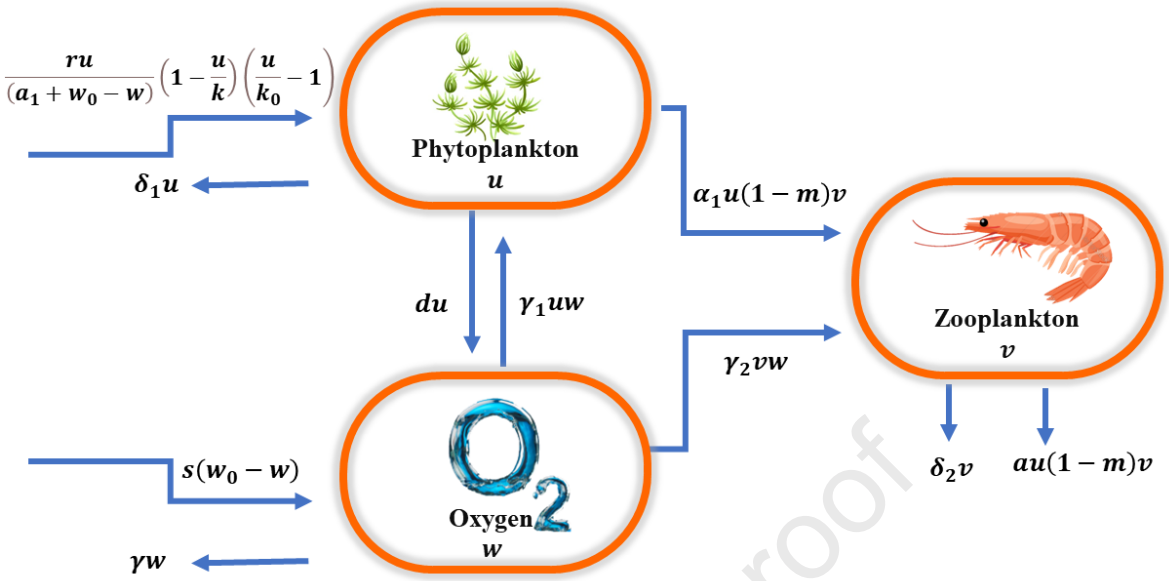

Figure 1: Schematic diagram of the DOPZ model.

In addition, the equations of the DOPZ model are $C^1(R_+^3)$, where $R_+^3 = \{(u, v, w), u \geq 0, v \geq 0, w \geq 0\}$. Therefore, they can be represented as Lipschitzian [27]. Thus, the solution of the DOPZ model exists, and it is unique.

3. Dynamical Evaluation Results

In this section, the well-posedness of the system and present conclusions about the presence of potential equilibrium points are discussed. in addition, the analysis of stability and bifurcation around the potential equilibrium points is examined.

3.1 Positivity and Boundedness

Since we are working with a biological system, the solutions of the DOPZ are essential to be both positive and bounded. The boundedness of solutions indicates that none of the populations exhibit unlimited growth. The quality of being bound is a crucial aspect of the system's proper functioning, as available resources limit it.

Theorem 1. All solutions of the DOPZ model $u(t), v(t)$ and $w(t)$ with the initial conditions $(u_{00}, v_{00}, w_{00}) \in R_+^3$ are positively invariant.

Proof: By integrating the first and second functions of the DOPZ model for $u(t)$ and $v(t)$ with a positive initial condition (u_{00}, v_{00}, w_{00}), we obtain

$$u(t) = u_{00}\, exp\left\{\int_0^t \left[\frac{r}{(a_1 + w_0 - w(\tau))}\left(1 - \frac{u(\tau)}{k}\right)\left(\frac{u(\tau)}{k_0} - 1\right) - \alpha_1(1-m)v(\tau) - \delta_1\right] d\tau\right\}$$

$$v(t) = v_{00}\, exp\left\{\int_0^t \left[\frac{\alpha_2(1-m)u(\tau)}{(a_2 + w_0 - w(\tau))} - \delta_2 - a(1-m)u(\tau)\right] d\tau\right\}$$

Then,

$$dw = (sw_0 + du - w(s + \gamma + \gamma_1 u + \gamma_2 v)dt$$

$$dw = \left[\begin{array}{c} sw_0 + du_{00}e^{\int_0^t\left[\frac{r}{(a_1+w_0-w(\tau))}\left(1-\frac{u(\tau)}{k}\right)\left(\frac{u(\tau)}{k_0}-1\right)-\alpha_1(1-m)v(\tau)-\delta_1\right]d\tau} \\ -w\left(\begin{array}{c} \mathrm{s} + \gamma + cv\gamma_1 u_{00}e^{\int_0^t\left[\frac{r}{(a_1+w_0-w(\tau))}\left(1-\frac{u(\tau)}{k}\right)\left(\frac{u(\tau)}{k_0}-1\right)-\alpha_1(1-m)v(\tau)-\delta_1\right]d\tau} \\ -\gamma_2 v_{00}e^{\int_0^t\left[\frac{\alpha_2(1-m)u(\tau)}{(a_2+w_0-w(\tau))}-\delta_2-a(1-m)u(\tau)\right]d\tau} \end{array}\right) \end{array}\right] dt$$

Therefore, after eliminating the non-negative terms, this produces

$$dw \geq \left[-\mathrm{w}\left(\begin{array}{c} \mathrm{s} + \gamma + \gamma_1 u_{00}e^{\int_0^t\left[\frac{r}{(a_1+w_0-w(\tau))}\left(1-\frac{u(\tau)}{k}\right)\left(\frac{u(\tau)}{k_0}-1\right)-\alpha_1(1-m)v(\tau)-\delta_1\right]d\tau} \\ +\gamma_2 v_{00}e^{\int_0^t\left[\frac{\alpha_2(1-m)u(\tau)}{(a_2+w_0-w(\tau))}-\delta_2-a(1-m)u(\tau)\right]d\tau} \end{array}\right)\right] dt$$

Consequently, by integrating the equation shown above for $w(t)$, these yields

$$w(t) \geq w_{00} exp\left\{\int_0^t \left[-\left(\begin{array}{c} \mathrm{s} + \gamma + \gamma_1 u_{00}e^{\int_0^{\bar{t}}\left[\frac{r}{(a_1+w_0-w(\tau))}\left(1-\frac{u(\tau)}{k}\right)\left(\frac{u(\tau)}{k_0}-1\right)-\alpha_1(1-m)v(\tau)-\delta_1\right]d\tau} \\ +\gamma_2 v_{00}e^{\int_0^{\bar{t}}\left[\frac{\alpha_2(1-m)u(\tau)}{(a_2+w_0-w(\tau))}-\delta_2-a(1-m)u(\tau)\right]d\tau} \end{array}\right)\right] d\bar{t}\right\}$$

As a result of the exponential function's definition, any solution, any solution $(u(t), v(t), w(t))$ that starts inside of R_+^3 with positive initial conditions (u_{00}, v_{00}, w_{00}) will remain in R_+^3. □

Theorem 2. Assume that $\alpha_1 \geq \alpha_2 + a$, then all solutions $u(t), v(t)$ and $w(t)$ of the DOPZ model that initiates in $\zeta = \left\{(u, v, w) \in R_+^3, u + v \leq \frac{kr(k+k_0)}{\delta k_0}, w \leq \frac{sw_0+kd}{s+\gamma}\right\}$, where $\delta = min\{\delta_1 + r,\ \delta_2,\}$, are uniformly bounded.

Proof: From the last equation of the DOPZ model, we obtain.

$$\frac{dw}{dt} \leq sw_0 + kd - (s + \gamma)w,$$

where k is the maximal phytoplankton carrying capacity. Now, by applying the separation of variables method, the following is obtained:

$$0 \leq w(t) \leq \frac{sw_0 + kd}{s+\gamma}\left(1 - e^{-(s+\gamma)t}\right) + w(0)e^{-(s+\gamma)t}$$

Hence,

$$0 \leq \lim_{t\to\infty} \sup w(t) \leq \frac{sw_0 + kd}{s+\gamma} = \mathcal{g}.$$

Let $L = u + v$, then

$$\frac{dL}{dt} = \frac{du}{dt} + \frac{dv}{dt}$$

Using the above dissolved oxygen bound and the fact that $\alpha_1 \geq \alpha_2 + a$, the following is obtained

$$\frac{dL}{dt} \leq \frac{ru}{(a_1 + w_0 - \mathcal{g})}\left(1 - \frac{u}{k}\right)\left(\frac{u}{k_0} - 1\right) - \alpha_1 u(1-m)v - \delta_1 u + \frac{\alpha_2 u(1-m)v}{(a_2 + w_0 - \mathcal{g})} - \delta_2 v - auv(1-m)$$

i.e.,

$$\frac{dL}{dt} \leq \frac{ru}{(a_1 + w_0 - \mathcal{g})}\left(1 - \frac{u}{k}\right)\left(\frac{u}{k_0} - 1\right) - \delta_1 u - \delta_2 v$$

By using the maximal phytoplankton carrying capacity k the following is obtained:

$$\frac{dL}{dt} \leq \frac{kr(k+k_0)}{k_0} - (\delta_1 + r)u - \delta_2 v$$

$\frac{dL}{dt} + \delta L \leq \frac{kr(k+k_0)}{k_0}$, where $\delta = min.\{\delta_1 + r,\ \delta_2\}$. Then applying Gronwall's inequality [28], the following is obtained:

$$0 \leq L\big(u(t), v(t)\big) \leq \frac{kr(k+k_0)}{\delta k_0}\left(1 - e^{-\delta t}\right) + L(0)e^{-\delta t},$$

hence,

$$0 \leq \lim_{t\to\infty} sup\ L(t) \leq \frac{kr(k+k_0)}{\delta k_0}.$$

So, $u(t), v(t)$ and $w(t)$ will remain bounded. □

Remark 1. Since α_1 indicates phytoplankton depletion owing to zooplankton intake and α_2 and a represent growth and the predation rate of toxic phytoplankton due to plankton interaction respectively, it is logical to conclude that

$$\alpha_1 \geq \alpha_2 + a.$$

Since we are dealing with a nonlinear system it is not easy to solve the proposed system directly. So the better way to understand the behavior of a non-linear system is to study the stability and the possible accruing of a bifurcation near the possible equilibrium points [29].

3.2 Existence of equilibria

The DOPZ model has the following steady states:

1. The dissolved oxygen equilibrium point (DOEP) is given by $F_1 = (0,0,\widehat{w})$, where $\widehat{w} = \frac{sw_0}{s+\gamma}$.
2. The zooplankton free equilibrium point (ZFEP) given by $F_2 = (\bar{u}, 0, \bar{w})$, where $\bar{w} = \frac{sw_0+du}{s+\gamma+\gamma_1 u} > 0$ and u is the root of the following equation:

$$g(u) = A_1u^3 + A_2u^2 + A_3u + A_4,$$

where $A_1 = \gamma_1 r$; $A_2 = r(s+\gamma) - \gamma_1 r(k+k_0)$;

$A_3 = -r(k+k_0)(s+\gamma) - \delta_1 kk_0 d + kk_0\gamma_1(sa_1 + sw_0 + r)$;

$A_4 = kk_0[(r+\delta_1 a_1)(s+\gamma) + \delta_1 w_0\gamma]$.

Clearly, $g(0) = kk_0[(r+\delta_1 a_1)(s+\gamma) + \delta_1 w_0\gamma] > 0$, and

$$g(k) = r^2\big(r(\gamma+s) - r\gamma_1(k+k_0)\big) - r(r(k+k_0)(\gamma+s) - kk_0\gamma_1(r + sa_1 + sw_0) + dkk_0\delta_1) + r^4\gamma_1 + kk_0\big((\gamma+s)(r+a_1\delta_1) + \gamma\delta_1 w_0\big).$$

Therefore, by the intermediate value theorem [30], $g(u)$ has a positive root say $u = \bar{u}$ in the interval $(0,k)$ if $g(k) < 0$.

3. The coexisting equilibrium point (CEP) given by $F_3 = (u^*, v^*, w^*)$, where $u^* = \frac{\delta_2(a_2+w_0-w^*)}{(1-m)[\alpha_2 - a(a_2+w_0-w^*)]}$, $v^* = \frac{r(k+k_0)u^* - r{u^*}^2 - rkk_0 - \delta_1 kk_0(a_1+w_0-w^*)}{\alpha_1(1-m)(a_1+w_0-w^*)kk_0}$, and w^* is the root of the following equation:

$$B_0w^5 + B_1w^4 + B_2w^3 + B_3w^2 + B_4w + B_5 = 0, \quad (2)$$

where, $B_i, i = 1,2,3,4,5$ are listed in the Appendix section. Using Descartes's rule of sign [31], Equation (2) has a unique positive root, if one of the following sets conditions hold:

$$B_0 > 0 \text{ and } B_{2,3,4,5} < 0,$$
$$B_{0,1} > 0 \text{ and } B_{3,4,5} < 0,$$
$$B_{0,1,2} > 0 \text{ and } B_{4,5} < 0,$$
$$B_{0,1,2,3} > 0 \text{ and } B_5 < 0,$$

$$\begin{aligned} &B_0 < 0 \text{ and } B_{2,3,4,5} > 0, \\ &B_{0,1} < 0 \text{ and } B_{,3,4,5} > 0, \\ &B_{0,1,2} < 0 \text{ and } B_{4,5} > 0, \\ &B_{0,1,2,3} < 0 \text{ and } B_5 > 0, \end{aligned} \tag{3}$$

For $u^*$and $v^*$to be positive, the following two conditions must be satisfied:

$$\begin{aligned} \alpha_2 &> a(a_2 + w_0 - w^*), \\ r(k + k_0)u^* &> ru^{*2} + rkk_0 + \delta_1 kk_0(a_1 + w_0 - w^*). \end{aligned} \tag{4}$$

3.3 Local Stability

The feature of the eigenvalues of the Jacobian matrix $J(u, v, w)$ at an equilibrium point is directly related to the behaviour of the DOPZ model near an equilibrium [32]. The $J(u, v, w)$ of the DOPZ model at any point, say (u, v, w), can be written as:

$$J = \begin{bmatrix} \frac{\partial f_1}{\partial u} & \frac{\partial f_1}{\partial v} & \frac{\partial f_1}{\partial w} \\ \frac{\partial f_2}{\partial u} & \frac{\partial f_2}{\partial v} & \frac{\partial f_2}{\partial w} \\ \frac{\partial f_3}{\partial u} & \frac{\partial f_3}{\partial v} & \frac{\partial f_3}{\partial w} \end{bmatrix} = (a_{ij})_{3\times 3},$$

where, $a_{11} = \frac{2ru(k+k_0)-3ru^2-rkk_0}{(a_1+w_0-w)kk_0} - \alpha_1 v(1-m) - \delta_1 \quad a_{12} = -\alpha_1 u(1-m); \quad a_{13} = \frac{ru^2(k+k_0)-ru^3-rkk_0u}{(a_1+w_0-w)^2k^2k_0^2}; a_{21} = \frac{\alpha_2 v(1-m)}{(a_2+w_0-w)} - av(1-m); a_{22} = \frac{\alpha_2 u(1-m)}{(a_2+w_0-w)} - \delta_2 - au(1-m); a_{23} = \frac{\alpha_2 u(1-m)v}{(a_2+w_0-w)^2}; a_{31} = d - \gamma_1 w; a_{32} = -\gamma_2 w; a_{33} = -(s + \gamma + \gamma_1 u + \gamma_2 v).$

Keeping this in mind, we take a look at the DOPZ system around each equilibrium:

1. The Jacobian matrix at the DOEP $F_1 = (0,0,\widehat{w})$ is given as:

$$J(F_1) = \begin{bmatrix} \frac{-r}{(a_1 + w_0 - \widehat{w})} - \delta_1 & 0 & 0 \\ 0 & -\delta_2 & 0 \\ d - \gamma_1 \widehat{w} & -\gamma_2 \widehat{w} & -s - \gamma \end{bmatrix} \tag{5}$$

Then, $J(F_1)$ has the eigenvalues $\lambda_{11} = \frac{-r}{(a_1+w_0-\widehat{w})} - \delta_1 < 0$, $\lambda_{12} = -\delta_2 < 0$, and $\lambda_{13} = -s - \gamma < 0$, which means F_1 is a locally asymptotically stable point.

2. The Jacobian matrix at the ZFEP $F_2 = (\bar{u}, 0, \bar{w})$ is given as:

$$J(F_2) = \begin{bmatrix} a_{11}^{[2]} & a_{12}^{[2]} & a_{13}^{[2]} \\ a_{21}^{[2]} & a_{22}^{[2]} & a_{23}^{[2]} \\ a_{31}^{[2]} & a_{32}^{[2]} & a_{33}^{[2]} \end{bmatrix}, \tag{6}$$

where $a_{11}^{[2]} = \frac{2r\bar{u}(k+k_0)-3r\bar{u}^2-rkk_0}{(a_1+w_0-\bar{w})kk_0}$; $a_{12}^{[2]} = -\alpha_1\bar{u}(1-m), a_{13}^{[2]} = \frac{r\bar{u}^2(k+k_0)-r\bar{u}^3-rkk_0\bar{u}}{(a_1+w_0-\bar{w})^2k^2k_0^2}$, $a_{21}^{[2]} = 0$; $a_{22}^{[2]} = \frac{\alpha_2\bar{u}(1-m)}{(a_2+w_0-\bar{w})} - \delta_2 - a\bar{u}(1-m)$; $a_{23}^{[2]} = 0$; $a_{31}^{[2]} = d - \gamma_1\bar{w}$; $a_{32}^{[2]} = -\gamma_2\bar{w}$; $a_{33}^{[2]} = -s - \gamma - \gamma_1\bar{u}$.

Then, the characteristic equation of $J(F_2)$ is given by:

$$\left(\frac{\alpha_2\bar{u}(1-m)}{(a_2+w_0-\bar{w})} - \delta_2 - a\bar{u}(1-m) - \lambda\right)\left[\lambda^2 - Tr\big(J(F_2)\big)\lambda + Det\big(J(F_2)\big)\right]$$

The eigenvalues of the above equation can be written as follows

$\lambda_{21} = \frac{\alpha_2\bar{u}(1-m)}{(a_2+w_0-\bar{w})} - \delta_2 - a\bar{u}(1-m)$,

$Tr\big(J(F_2)\big) = \frac{\left[2r\bar{u}(k+k_0)-3r\bar{u}^2-rkk_0\right]-(s+\gamma+\gamma_1\bar{u})(a_1+w_0-\bar{w})kk_0}{(a_1+w_0-\bar{w})kk_0}$,

$Det\big(J(F_2)\big) = \frac{\left[2r\bar{u}(k+k_0)-3r\bar{u}^2-rkk_0\right][-s-\gamma-\gamma_1\bar{u}]}{(a_1+w_0-\bar{w})kk_0} - \left[\frac{r\bar{u}^2(k+k_0)-3\bar{u}^3-rkk_0\bar{u}}{(a_1+w_0-\bar{w})^2k^2k_0^2}\right][d-\gamma_1\bar{w}]$.

Clearly, F_2 exhibits local asymptotic stability if and only if the following conditions are fulfilled:

$$\left.\begin{array}{c} \delta_2 + a\bar{u}(1-m) > \frac{\alpha_2\bar{u}(1-m)}{(a_2+w_0-\bar{w})}, \\ 2r\bar{u}(k+k_0) < 3r\bar{u}^3 + rkk_0 + (s+\gamma+\gamma_1\bar{u})(a_1+w_0-\bar{w})kk_0, \\ Det\big(J(F_2)\big) > 0. \end{array}\right\} \tag{7}$$

3. The Jacobian matrix at the CEP $F_3 = (u^*, v^*, w^*)$ is given as:

$$J(F_3) = \begin{bmatrix} a_{11}^{[3]} & a_{12}^{[3]} & a_{13}^{[3]} \\ a_{21}^{[3]} & a_{22}^{[3]} & a_{23}^{[3]} \\ a_{31}^{[3]} & a_{32}^{[3]} & a_{33}^{[3]} \end{bmatrix}. \tag{8}$$

where, $a_{11}^{[3]} = \frac{2ru^*(k+k_0)-3ru^{*2}-rkk_0}{(a_1+w_0-w^*)kk_0} - \delta_1 - \alpha_1v^*(1-m)$; $a_{12}^{[3]} = -\alpha_1u^*(1-m)$; $a_{13}^{[3]} = \frac{ru^{*2}(k+k_0)-ru^{*3}-rkk_0u^*}{(a_1+w_0-w^*)^2k^2k_0^2}$; $a_{21}^{[3]} = \frac{\alpha_2v^*(1-m)}{(a_2+w_0-w^*)} - av^*(1-m)$; $a_{22}^{[3]} = 0$, $a_{23}^{[3]} = \frac{\alpha_2u^*(1-m)v^*}{(a_2+w_0-w^*)^2}$;; $a_{31}^{[3]} = d-\gamma_1w^*$; $a_{32}^{[3]} = -\gamma_2w^*$; $a_{33}^{[3]} = -s-\gamma-\gamma_1u^*-\gamma_2v^*$.

Therefore, the characteristic equation of $J(F_3)$ is represented as:

$$\lambda^3 + A_1\lambda^2 + A_2\lambda + A_3 = 0, \tag{9}$$

where,

$A_1 = -\left(a_{11}^{[3]} + a_{33}^{[3]}\right)$,

$A_2 = -(a_{13}^{[3]}a_{31}^{[3]} + a_{23}^{[3]}a_{32}^{[3]} + a_{12}^{[3]}a_{21}^{[3]} - a_{11}^{[3]}a_{33}^{[3]})$,

$A_3 = a_{11}^{[3]}a_{23}^{[3]}a_{32}^{[3]} + a_{12}^{[3]}a_{21}^{[3]}a_{33}^{[3]} - a_{13}^{[3]}a_{21}^{[3]}a_{32}^{[3]} - a_{12}^{[3]}a_{23}^{[3]}a_{31}^{[3]}$,

$\Delta = A_1A_2 - A_3 = \left(a_{11}^{[3]} + a_{33}^{[3]}\right)\left(a_{13}^{[3]}a_{31}^{[3]} - a_{11}^{[3]}a_{33}^{[3]}\right) + a_{11}^{[3]}a_{12}^{[3]}a_{21}^{[3]} + a_{23}^{[3]}a_{32}^{[3]}a_{33}^{[3]} + a_{12}^{[3]}a_{23}^{[3]}a_{31}^{[3]} + a_{13}^{[3]}a_{21}^{[3]}a_{32}^{[3]}$.

Now, from the Routh-Hurwitz criteria [32], F_3 is a LAS point, under the condition that $A_1 > 0, A_3 > 0$ and $\Delta > 0$.

In the following theorem, adequate conditions for the global stability of the CEP, which is given by $F_3 = (u^*, v^*, w^*)$ are identified by the Lyapunov method [33].

Theorem 3. Assume that

$$\left.\begin{aligned} [d + w^*]^2 &\le \tfrac{4c_1 r}{kk_0}[(u + u^*) - (k + k_0)][s + \gamma + \gamma_1 u + \gamma_2 v] \\ w^*(v - v^*)(w - w^*) &< \left[\sqrt{\tfrac{c_1 r}{kk_0}[(u + u^*) - (k + k_0)]} + \sqrt{s + \gamma + \gamma_1 u + \gamma_2 v}\right]^2 \\ \alpha_2 &> a \end{aligned}\right\} \tag{10}$$

then CEP is globally asymptotically stable in R_+^3.

Proof: Define $G_3 = c_1\left(u - u^* - u^* \ln\frac{u}{u^*}\right) + c_2\left(v - v^* - v^* \ln\frac{v}{v^*}\right) + c_3\left(\frac{w-w^*}{2}\right)^2$, where c_1, c_2 and c_3 are positive constants to be specified and $G_3(u, v, w)$ is a positive definite function of CEP. Thus,

$$\frac{dG_3}{dt} \le c_1(u - u^*)\left[-\frac{ru^2}{kk_0} + \frac{r(k+k_0)u}{kk_0} - r + \frac{ru^{*2}}{kk_0} - \frac{r(k+k_0)u^*}{kk_0} + r - \alpha_1(1 - m)(v - v^*\right] + c_2(v - v^*)[(\alpha_2 - a)(1 - m)(u - u^*)] + c_3(w - w^*)\left[-(s + \gamma)(w - w^*) + d(u - u^*) - \gamma_1 u(w - w^*) + w^*(u - u^*) - \gamma_2 v(w - w^*) + w^*(v - v^*)\right]$$

Therefore,

$$\begin{aligned} \frac{dG_3}{dt} \le &-\frac{c_1 r(u - u^*)^2}{kk_0}[(u + u^*) - (k + k_0)] - (1 - m)(u - u^*)(v - v^*)[c_1\alpha_1 - c_2\alpha_2 + c_2 a] \\ &- c_3(w - w^*)^2[(s + \gamma) + \gamma_1 u + \gamma_2 v] + c_3(u - u^*)(w - w^*)[d + w^*] \\ &+ c_3 w^*(v - v^*)(w - w^*) \end{aligned}$$

By choosing the constants as: $c_2 = c_3 = 1$ and $c_1 = \frac{(\alpha_2 - a)}{\alpha_1}$, the following is obtained,

$$\frac{dG_3}{dt} \leq -\frac{c_1 r}{kk_0}[(u+u^*)-(k+k_0)](u-u^*)^2 + [d+w^*](u-u^*)(w-w^*) - [(s+\gamma)+\gamma_1 u+\gamma_2 v](w-w^*)^2 + w^*(v-v^*)(w-w^*).$$

After some algebraic computation, we obtain

$$\frac{dG_3}{dt} \leq -\left[\sqrt{\frac{c_1 r}{kk_0}[(u+u^*)-(k+k_0)]}(u+u^*) + \sqrt{s+\gamma+\gamma_1 u+\gamma_2 v}(w-w^*) + w^*(v-v^*)(w-w^*)\right]^2$$

Then, $\frac{dG_3}{dt} < 0$ under condition (10). Hence, G_3 is a Lyapunov function. Therefore, CEP is globally asymptotically stable in R_+^3 if u, v and w are controlled as in condition (10).

3.4 Local Bifurcation

Bifurcation theory looks at how the structure of a group of curves, like the solutions to a set of differential equations, can change over time. A bifurcation happens when a small, smooth change in the values of a system's parameters causes a big change in the way it acts. It is most often used in mathematics to study systems that change over time. Local bifurcations happen when parameters cross critical thresholds and cause changes in the local stability of equilibria. In this section, it is checked to see if there is a chance of local bifurcation. See [27] and [34] for a comprehensive treatment. To this end, we rewrite the DOPZ model as follows:

$$\frac{dU}{dt} = F(U), \text{ with } U = \begin{pmatrix} u \\ v \\ w \end{pmatrix}, \text{ and } F = \begin{pmatrix} f_1(u,v,w) \\ f_2(u,v,w) \\ f_3(u,v,w) \end{pmatrix}.$$

For a nonzero vector $Z = (z_1, z_2, z_3)^T$ we set

$$D^2F(z,z) = \begin{bmatrix} c_{11} \\ c_{21} \\ c_{31} \end{bmatrix}, \tag{11}$$

where,

$c_{11} = \frac{[2r(k+k_0)-6ru]z_1^2}{(a_1+w_0-w)kk_0} - 2\alpha_1(1-m)z_1z_2 + \left[\frac{2ru(k+k_0)-3ru^2-rkk_0}{(a_1+w_0-w)^2}\right]\left[z_1z_3 + \frac{z_1z_3}{k^2k_0^2}\right] + \left[\frac{2ru^2(k+k_0)-2ru^3-2rkk_0u}{(a_1+w_0-w)^3k^2k_0^2}\right]$,

$c_{21} = \frac{2\alpha_2(1-m)}{(a_2+w_0-w)}\left[z_1z_2 - \frac{uvz_3^2}{(a_2+w_0-w)^2}\right] - 2a(1-m)z_1z_2$,

$c_{31} = -2\gamma_1 z_1 z_3 - 2\gamma_2 z_2 z_3$.

Theorem 4. For $\alpha_2^* = \frac{[\delta_2 + a\bar{u}(1-m)](a_2 + w_0 - \bar{w})}{\bar{u}(1-m)}$, the DOPZ model, at F_2 has

1) no saddle-node bifurcation.
2) a transcritical bifurcation if
$$\left(P^{[2]}\right)^T \left[D^2 F(F_2, \alpha_2^*)\left(Z^{[2]}, Z^{[2]}\right)\right] \neq 0. \tag{12}$$
3) a pitchfork bifurcation if condition (12) is violated and the following statement is satisfied
$$\left(P^{[2]}\right)^T \left[D^3 F(F_2, \alpha_2^*)\left(Z^{[2]}, Z^{[2]}, Z^{[2]}\right)\right] \neq 0, \tag{13}$$

where the notation in (12) and (13) will be introduced during the proof.

Proof: - At $\alpha_2^* = \frac{[\delta_2 + a\bar{u}(1-m)](a_2 + w_0 - \bar{w})}{\bar{u}(1-m)}$, $J(F_2)$ has a zero eigenvalue $\lambda_{21} = 0$. Therefore, $J(F_2)$ at α_2^* becomes

$$J^*(F_2) = \begin{bmatrix} \frac{2r\bar{u}(k+k_0) - 3r\bar{u}^2 - rkk_0}{(a_1 + w_0 - w)kk_0} - \delta_1 & -\alpha_1 k & \frac{r\bar{u}^2(k+k_0) - r\bar{u}^3 - rkk_0\bar{u}}{T_2^2 k^2 k_0^2} \\ 0 & 0 & 0 \\ d - \gamma_1\bar{w} & -\gamma_2\bar{w} & -s - \gamma - \gamma_1\bar{u} \end{bmatrix}.$$

Now, let $Z^{[2]} = \left(z_1^{[2]}, z_2^{[2]}, z_3^{[2]}\right)^T$ be an eigenvector corresponding to $\lambda_{21} = 0$. Thus $(J^*(F_2) - \lambda_{21} I)Z^{[2]} = 0$, which gives:

$z_1^{[2]} = \frac{[\alpha_1\bar{u}(1-m)e_1 e_3^2 + e_2\gamma_2\bar{w}]z_2^{[2]}}{[(e_4 - \gamma_1 e_3)e_1 e_3 + e_2(d - \gamma_1\bar{w})]kk_0}$, $z_3^{[2]} = \frac{(d-\gamma_1\bar{w})z_1^{[2]} - \gamma_2\bar{w}z_2^{[2]}}{s+\gamma+\gamma_1\bar{u}}$ and $z_2^{[2]}$ represents any nonzero real number, where $(e_4 - \gamma_1 e_3)e_1 e_3 + e_2(d - \gamma_1\bar{w}) \neq 0$ and

$e_1 = s + \gamma + \gamma_1\bar{u}$; $e_2 = r\bar{u}^2(k + k_0) - r\bar{u}^3 - rkk_0\bar{u}$; $e_3 = (a_1 + w_0 - \bar{w})kk_0$; $e_4 = 2r\bar{u}(k + k_0) - 3r\bar{u}^2 - rkk_0$. That means

$$Z^{[2]} = \left(\frac{[\alpha_1\bar{u}(1-m)e_1 e_3^2 + e_2\gamma_2\bar{w}]z_2^{[2]}}{[(e_4 - \gamma_1 e_3)e_1 e_3 + e_2(d - \gamma_1\bar{w})]kk_0}, z_2^{[2]}, \frac{(d-\gamma_1\bar{w})z_1^{[2]} - \gamma_2\bar{w}z_2^{[2]}}{s+\gamma+\gamma_1\bar{u}}\right)^T.$$

Let $P^{[2]} = \left(p_1^{[2]}, p_2^{[2]}, p_3^{[2]}\right)^T$ be an eigenvector associated with $\lambda_{21} = 0$ of the matrix J_2^{*T}. Then $(J_2^{*T} - \lambda_{21} I)P^{[2]} = 0$. By solving this equation for $P^{[2]}$, $P^{[2]} = \left(p_1^{[2]}, p_2^{[2]}, \frac{r\bar{u}^2(k+k_0) - r\bar{u}^3 - rkk_0\bar{u}}{(a_1 + w_0 - \bar{w})^2 k^2 k_0^2 (s+\gamma+\gamma_1\bar{u})}\right)^T$ is obtained, where $p_1^{[2]}$ and $p_2^{[2]}$ is any nonzero real number.

Then, the following is taken into account to check if saddle-node bifurcation meets the criteria of Sotomayor's theorem [35]:

$$\frac{\partial F}{\partial \alpha_2} = F_{\alpha_2}(F_2, \alpha_2) = \left(\frac{\partial f_1}{\partial \alpha_2}, \frac{\partial f_2}{\partial \alpha_2}, \frac{\partial f_3}{\partial \alpha_2}\right)^T = \left(0, \frac{uv(1-m)}{(a_2 + w_0 - w)}, 0\right)^T.$$

So, $F_{\alpha_2}(F_2, \alpha_2^*) = (0,0,0)^T$.

Therefore, the first criterion for transcritical bifurcation or pitchfork bifurcation holds, whilst saddle-node bifurcation cannot arise. Subsequently,

$$DF_{\alpha_2}(F_2, \alpha_2^*) = \begin{bmatrix} 0 & 0 & 0 \\ 0 & \dfrac{\bar{u}(1-m)}{(a_2 + w_0 - \bar{w})} & 0 \\ 0 & 0 & 0 \end{bmatrix}$$

where, $DF_{\alpha_2}(S, \alpha_2)$ represents the derivative of $F_{\alpha_2}(S, \alpha_2)$ with respect to $S = (u, v, w)^T$. Furthermore,

$$DF_{\alpha_2}(F_2, \alpha_2^*)Z^{[2]} = \begin{bmatrix} 0 & 0 & 0 \\ 0 & \dfrac{\bar{u}(1-m)}{(a_2 + w_0 - \bar{w})} & 0 \\ 0 & 0 & 0 \end{bmatrix} \begin{bmatrix} z_1^{[2]} \\ z_2^{[2]} \\ z_3^{[2]} \end{bmatrix}$$

$$\left(P^{[2]}\right)^T DF_{\alpha_2}(F_2, \alpha_2^*)Z^{[2]} = \left(p_1^{[2]}, p_2^{[2]}, p_3^{[2]}\right)\left(0, \frac{\bar{u}(1-m)z_2^{[2]}}{(a_2+w_0-\bar{w})}, 0\right)^T = \frac{\bar{u}(1-m)z_2^{[2]}p_2^{[2]}}{(a_2+w_0-\bar{w})} \neq 0.$$

Therefore, the second condition for transcritical or pitchfork bifurcation holds.

Next, we assume that condition (12) holds, i.e.

$$\left(P^{[2]}\right)^T \left[D^2F(F_2, \alpha_2^*)\left(Z^{[2]}, Z^{[2]}\right)\right] \neq 0.$$

This implies that the necessary conditions for a transcritical bifurcation are met.

Finally, if condition (12) is not satisfied, then the first, second and third conditions of pitchfork bifurcation are satisfied according to Sotomayor's theorem. Further, we have

$$D^3F(z, z, z) = \begin{bmatrix} x_{11} \\ x_{21} \\ x_{31} \end{bmatrix},$$

where,

$x_{11} = -\frac{6rz_1^3}{(a_1+w_0-w)kk_0} + \left[\frac{2r(k+k_0)-6ru}{(a_1+w_0-w)^2}\right]\left[2z_1^2z_3 + \frac{z_1^2z_3}{k^2k_0^2}\right] + \left[\frac{4ru(k+k_0)-6ru^2-2rkk_0}{(a_1+w_0-w)^3}\right]\left[z_1z_3^2 + \frac{2z_1z_3^2}{k^2k_0^2}\right] + \frac{6ru\left[u(k+k_0)-u^2-kk_0\right]z_3^2}{(a_1+w_0-w)^4k^2k_0^2}$;

$x_{21} = \frac{2\alpha_2(1-m)z_3}{(a_2+w_0-w)^2}\left[z_1z_2 - \frac{vz_1z_3}{(a_2+w_0-w)} - \frac{uz_2z_3}{(a_2+w_0-w)} - \frac{3uvz_3^2}{(a_2+w_0-w)^2}\right]$; $x_{31} = 0$.

Hence,

$$\left(P^{[2]}\right)^T\left[D^3F(F_2,\alpha_2^*)\left(Z^{[2]},Z^{[2]},Z^{[2]}\right)\right] = \left(p_1^{[2]},p_2^{[2]},p_3^{[2]}\right)\left(-\frac{6r\left[z_1^{[2]}\right]^3}{(a_1+w_0-\bar{w})kk_0}+\right.$$

$$\left[\frac{2r(k+k_0)-6r\bar{u}}{(a_1+w_0-\bar{w})^2}\right]\left[2\left[z_1^{[2]}\right]^2 z_3^{[2]}+\frac{\left[z_1^{[2]}\right]^2 z_3^{[2]}}{k^2k_0^2}\right]+\left[\frac{4r\bar{u}(k+k_0)-6r\bar{u}^2-2rkk_0}{(a_1+w_0-\bar{w})^3}\right]\left[z_1^{[2]}\left[z_3^{[2]}\right]^2+\frac{2z_1^{[2]}\left[z_3^{[2]}\right]^2}{k^2k_0^2}\right]+$$

$$\frac{6r\bar{u}\left[\bar{u}(k+k_0)-\bar{u}^2-kk_0\right]\left[z_3^{[2]}\right]^2}{(a_1+w_0-\bar{w})^4k^2k_0^2},\frac{2\delta_2+2a\bar{u}(1-m)}{(a_2+w_0-\bar{w})}\left.\left[z_1^{[2]}z_2^{[2]}z_3^{[2]}-\frac{z_2^{[2]}\left[z_3^{[2]}\right]^2}{k^2k_0^2}\right],0\right)^T.$$

$$=-\frac{6r\left[z_1^{[2]}\right]^3p_1^{[2]}}{(a_1+w_0-\bar{w})kk_0}+\left[\frac{2r(k+k_0)-6r\bar{u}}{(a_1+w_0-\bar{w})^2}\right]\left[2\left[z_1^{[2]}\right]^2 z_3^{[2]}+\frac{\left[z_1^{[2]}\right]^2 z_3^{[2]}}{k^2k_0^2}\right]p_1^{[2]}+$$

$$\left[\frac{4r\bar{u}(k+k_0)-6r\bar{u}^2-2rkk_0}{(a_1+w_0-\bar{w})^3}\right]\left[z_1^{[2]}\left[z_3^{[2]}\right]^2+\frac{2z_1^{[2]}\left[z_3^{[2]}\right]^2}{k^2k_0^2}\right]p_1^{[2]}+\frac{6r\bar{u}\left[\bar{u}(k+k_0)-\bar{u}^2-kk_0\right]\left[z_3^{[2]}\right]^2}{(a_1+w_0-\bar{w})^4k^2k_0^2}p_1^{[2]}+$$

$$\frac{2\delta_2+2a\bar{u}(1-m)}{(a_2+w_0-\bar{w})}\left[z_1^{[2]}z_2^{[2]}z_3^{[2]}-\frac{z_2^{[2]}\left[z_3^{[2]}\right]^2}{k^2k_0^2}\right]p_2^{[2]}.$$

This means if condition (13) is satisfied, then the DOPZ model has a pitchfork bifurcation at F_2 with the parameter α_2^*.

Theorem 5. For $\gamma_2^*=\frac{a_{11}^{[3]}\left(a_{13}^{[3]}a_{31}^{[3]}+a_{12}^{[3]}a_{21}^{[3]}+a_{11}^{[3]}a_{33}^{[3]}-\left[a_{33}^{[3]}\right]^2\right)+a_{13}^{[3]}\left[a_{31}^{[3]}a_{33}^{[3]}+a_{21}^{[3]}a_{32}^{[3]}\right]}{\left[a_{32}^{[3]}a_{33}^{[3]}+a_{12}^{[3]}a_{31}^{[3]}\right]w^*}$, where the formulas of $a_{ij}^{[3]}=d_{ij}$ are given in the following proof, the DOPZ model at CEP has a saddle-node bifurcation if

$$D^2F(F_3,\gamma_1^*)\left(Z^{[3]},Z^{[3]}\right)\neq 0. \tag{14}$$

Proof: - According to $J(F_3)$, given by (8), the DOPZ model at CEP has a zero eigenvalue, say $\lambda_{31}=0$, at $\gamma_2^*=\frac{a_{11}^{[3]}\left(a_{13}^{[3]}a_{31}^{[3]}+a_{12}^{[3]}a_{21}^{[3]}+a_{11}^{[3]}a_{33}^{[3]}-\left[a_{33}^{[3]}\right]^2\right)+a_{13}^{[3]}\left[a_{31}^{[3]}a_{33}^{[3]}+a_{21}^{[3]}a_{32}^{[3]}\right]}{\left[a_{32}^{[3]}a_{33}^{[3]}+a_{12}^{[3]}a_{31}^{[3]}\right]w^*}$, where $(a_{32}^{[3]}a_{33}^{[3]}+a_{12}^{[3]}a_{31}^{[3]})\neq 0$ and the Jacobian matrix $J^*(F_3)=J(F_3,\gamma_2^*)$, becomes:

$$J^*(F_3)=\begin{bmatrix}d_{11}&d_{12}&d_{13}\\d_{21}&d_{22}&d_{23}\\d_{31}&d_{32}&d_{33}\end{bmatrix}$$

$d_{11}=\frac{2ru^*(k+k_0)-3ru^{*2}-rkk_0}{(a_1+w_0-w^*)kk_0}-\alpha_1v(1-m)-\delta_1;$

$d_{12} = -\alpha_1 u^*(1-m);\ d_{13} = \frac{ru^{*2}(k+k_0) - ru^{*3} - rkk_0u^*}{(a_1+w_0-w^*)^2k^2k_0^2};\ d_{21} = \frac{\alpha_2 v^*(1-m)}{(a_2+w_0-w^*)} - av^*(1-m);\ d_{22} = 0;\ d_{23} = \frac{\alpha_2 u^*(1-m)v^*}{(a_2+w_0-w^*)^2};\ d_{31} = d - \gamma_1 w^*;\ d_{32} = -\gamma_2^* w^*;\ d_{33} = -s - \gamma - \gamma_1 u^* - \gamma_2^* v^*.$

Now, let $Z^{[3]} = \left(z_1^{[3]}, z_2^{[3]}, z_3^{[3]}\right)^T$ be an eigenvector corresponding to $\lambda_{31} = 0$. Thus $(J^*(F_3) - \lambda_{31}F)Z^{[3]} = 0$, which implies: $z_1^{[3]} = \frac{-d_{23}z_3^{[3]}}{d_{21}}, z_2^{[3]} = \frac{(d_{31}d_{23} - d_{21}d_{33})z_3^{[3]}}{d_{21}d_{23}}$, where $d_{21} \neq 0$ and $z_3^{[3]}$ represents any nonzero real number. That means $Z^{[3]} = \left(z_1^{[3]}, z_2^{[3]}, z_3^{[3]}\right)^T$.

Let $P^{[3]} = \left(p_1^{[3]}, p_2^{[3]}, p_3^{[3]}\right)^T$ be an eigenvector associated with $\lambda_{31} = 0$ of the matrix $J^*(F_3)$. Then $(J_3^{*T} - \lambda_{31}I)P^{[3]} = 0$. By solving this equation for $P^{[3]}$, $P^{[3]} = \left(\frac{-d_{32}P_3^{[3]}}{d_{12}}, \left[\frac{d_{13}d_{32}}{d_{12}d_{23}} - \frac{d_{33}}{d_{23}}\right]P_3^{[3]}, P_3^{[3]}\right)^T$ is obtained, where $P_3^{[3]}$ is any nonzero real number.

Now, the following are quantified to ensure that Sotomayor's theorem for saddle-node bifurcation holds:

$$\frac{\partial F}{\partial \gamma_2} = \left(\frac{\partial f_1}{\partial \gamma_2}, \frac{\partial f_2}{\partial \gamma_2}, \frac{\partial f_3}{\partial \gamma_2}\right)^T = (0,0,-vw)^T.$$

So, $F_{\gamma_2} = (F_3, \gamma_2^*) = (0,0,-v^*w^*)^T$ and hence $\left(P^{[3]}\right)^T F_{\gamma_2}(F_3, \gamma_2^*) = -v^*w^*p_3^{[3]} \neq 0$.

Hence, the first requirement for saddle-node bifurcation is satisfied, but transcritical or pitchfork bifurcation is not possible. Subsequently,

$$D^2F(F_3, \gamma_1^*)\left(Z^{[3]}, Z^{[3]}\right) = \left(\frac{2r(k+k_0) - 6ru^*\left[z_1^{[3]}\right]^2}{(a_1+w_0-w^*)kk_0} - 2\alpha_1(1-m)z_1^{[3]}z_2^{[3]} + \left[\frac{2ru^*(k+k_0) - 3ru^{*2} - rkk_0}{(a_1+w_0-w^*)^2}\right]\left[z_1^{[3]}z_3^{[3]} + \frac{z_1^{[3]}z_3^{[3]}}{k^2k_0^2}\right] + \frac{2ru^*\left[u^*(k+k_0) - u^{*2} - kk_0\right]\left[z_3^{[3]}\right]^2}{(a_1+w_0-w^*)^3k^2k_0^2}, \frac{2\alpha_2(1-m)}{(a_2+w_0-w^*)}\left[z_1^{[3]}z_2^{[3]} - \frac{u^*v^*\left[z_3^{[3]}\right]^2}{(a_1+w_0-w^*)^2}\right] - 2a(1-m)z_1^{[3]}z_2^{[3]}, -2\gamma_1 z_1^{[3]}z_3^{[3]} - 2\gamma_2^* z_2^{[3]}z_3^{[3]}\right)^T.$$

Hence, condition (14) guarantees that the second condition of saddle-node bifurcation is satisfied. Therefore, the DOPZ model has saddle-node bifurcation at CEP with the parameter γ_2^*.

From Theorem 6, the Bendixson–Dulac criterion [13] is used to find the conditions that guarantee the DOPZ model has no periodic behaviour (Hopf bifurcation) in the positive quadrant of the uw-plane.

Theorem 6: The DOPZ System has no periodic solution in $R^2_{+(u,w)}$, if one of the following conditions is true for all (u,w) in $R^2_{+(u,w)}$:

$$\begin{aligned}\frac{r(k+k_0)}{(a_1+w_0-w)kk_0w} &< \frac{2ur}{(a_1+w_0-w)kk_0w} + \frac{sw_0}{uw^2} + \frac{d}{w^2},\\ \frac{r(k+k_0)}{(a_1+w_0-w)kk_0w} &> \frac{2ur}{(a_1+w_0-w)kk_0w} + \frac{sw_0}{uw^2} + \frac{d}{w^2}.\end{aligned} \tag{15}$$

Proof: For any initial value (u,w) in $R^2_{+(u,w)}$, let $E(u,w) = \frac{1}{uw}$, $e_1(u,w) = u\left[\frac{r}{(a_1+w_0-w)}\left(1-\frac{u}{k}\right)\left(\frac{u}{k_0}-1\right)-\delta_1\right]$ and $e_2(u,w) = s(w_0-w)+du-\gamma w-\gamma_1 uw$.

Clearly, $E(u,w) > 0$ for all $(u,w) \in R^2_+$ and it is a C^1 function in $R^2_{+(u,w)} = \{(u,w), u>0, w>0,\}$.

Thus $\Delta(u,w) = \frac{\partial}{\partial u}(Ee_1) + \frac{\partial}{\partial w}(Ee_2) = \frac{-2ru+r(k+k_0)}{(a_1+w_0-w)kk_0w} - \frac{sw_0}{uw^2} - \frac{d}{w^2} < 0$. $\Delta(u,v)$ does not change sign if one of the inequalities given on (15) satisfies and it is not identically zero in $R^2_{+(u,w)}$. Therefore, the DOPZ model has no periodic dynamics in $R^2_{+(u,w)}$.

From Theorem 7, the steady state of ZFEP changes as the parameter γ crosses the threshold value γ^*, which implies that ZFEP may become unstable due to Hopf bifurcation when forced to operate within particular restrictions on its parameters. In the case where we use γ as the bifurcation parameter, the Hopf bifurcation threshold is the positive root of $Tr\,J(F_2)|_{\gamma=\gamma^*} = 0$, under the condition $Det\,J(F_2)|_{\gamma=\gamma^*} > 0$.

This leads us to the following theorem as a result.

Theorem 7. Assume that the third inequality of condition (7) holds along with the following condition:

$$\gamma^* > 0, \tag{16}$$

where γ^* is defined in the proof of the theorem. Then, the DOPZ model presents a Hopf bifurcation at $\gamma = \gamma^*$ around the ZFEP.

Proof: - The characteristic equation of matrix $J(F_2)$ is

$$\lambda^2 - Tr\big(J(F_2)\big)\lambda + Det\,J(F_2) = 0, \tag{17}$$

and the prerequisites for the occurrence of the Hopf bifurcation are outlined below.

a) $[Tr\, J(F_2)]|_{\gamma=\gamma^*} = 0$,
b) $[Det\, J(F_2)]|_{\gamma=\gamma^*} > 0$,
c) $\frac{d}{d\gamma}\left[Re\left(\lambda_{1,2}\right)\right]_{\gamma=\gamma^*} \neq 0$ (Transversality condition).

Conditions (a) and (b) have been satisfied at $\gamma^* = \frac{2r\bar{u}(k+k_0)-3r\bar{u}^2+rkk_0}{(a_1+w_0-\bar{w})kk_0} - (s+\gamma_1\bar{u})$. Clearly $\gamma^* > 0$ if Condition 16 holds. At $\gamma = \gamma^*$, the characteristic equation given by (17) is rewritten as $\lambda^2 + Det\, J(F_2) = 0$, which has two roots

$$\lambda_{1,2} = \pm i\sqrt{detJ(F_2)}.$$

Clearly, at $\gamma = \gamma^*$ there are two purely imaginary eigenvalues λ_1 and λ_2 which are complex conjugates under conditions (7).

Further, we write the general roots of equation (3) in the neighbourhood of γ^*as

$\lambda_{1,2} = \frac{tr\left(J(F_2)\right)\pm i\sqrt{detJ(F_2)}}{2}$, then $\frac{d}{d\gamma}[Re\left(\lambda_{1,2}\right)]_{\gamma=\gamma^*} = \frac{d}{d\gamma}\left[\frac{tr\left(J(F_2)\right)}{2}\right]_{\gamma=\gamma^*} = \frac{-1}{2} \neq 0.$

That means the third condition (c) has been verified, ensuring that when $\gamma = \gamma^*$, a Hopf bifurcation takes place at ZFEP.

In theorem 8, the existence of a Hopf bifurcation around CEP is discussed.

Theorem 8. Under the following assumptions

$$A_i > 0, i = 1,2 \quad (18)$$
$$a_{12}^{[3]}a_{23}^{[3]} - a_{13}^{[3]}A_1'(\gamma_1^*) \neq 0 \quad (19)$$
$$\gamma_1^* > 0. \quad (20)$$

Here, Ai's represent the coefficients of the characteristic equation that was mentioned in equation (9) with $\gamma_1 = \gamma_1^*$ and the formula for γ_1^* is given in the below proof. Then, there exists a Hopf bifurcation for CEP at $\gamma_1 = \gamma_1^*$.

Proof: - The value of the bifurcation parameter can be found if we set $A_1(\gamma_1^*)A_2(\gamma_1^*) - A_3(\gamma_1^*) = 0$ in equation (9). This gives:

$$\gamma_1^* = \frac{(d_{11}d_{13}+d_{13}d_{33}+d_{12}d_{23})d+d_{11}(d_{12}d_{21}-d_{11}d_{33}-d_{33}^2)+d_{32}(d_{23}d_{33}+d_{13}d_{21})}{(d_{11}d_{13}+d_{13}d_{33}+d_{12}d_{23})w^*}.$$

Clearly, $\gamma_1^* > 0$ if condition (20) holds. Now, at $\gamma_1 = \gamma_1^*$ Equation (9) can be written as

$$(\lambda + A_1)(\lambda^2 + A_2) = 0.$$

According to condition (18), the above equation has three roots, a negative root $\lambda_1 = -A_1$ and two purely imaginary roots $\lambda_{2,3} = \pm i\sqrt{A_2}$. In a neighbourhood of γ_1^*, the roots have the following forms: $\lambda_1 = -A_1, \lambda_{2,3} = \rho_1(\gamma_1) \pm i\rho_2(\gamma_1)$.

Clearly, $Re(\lambda_{2,3})|_{\gamma_1=\gamma_1^*} = \rho_1(\gamma_1^*) = 0$ indicates that the first condition for Hopf bifurcation has been met at $\gamma_1 = \gamma_1^*$. Now to confirm the transversality condition, we substitute $\rho_1(\gamma_1) \pm i\rho_2(\gamma_1)$ into equation (9) and then compute its derivative with respect to γ_1^*, $\Theta(\gamma_1^*)\psi(\gamma_1^*) + \Gamma(\gamma_1^*)\phi(\gamma_1^*) \neq 0$, where the form of $\Theta(\gamma_1^*), \psi(\gamma_1^*), \Gamma(\gamma_1^*)$ and $\phi(\gamma_1^*)$ are

$$\psi(\gamma_1) = 3\rho_1^2(\gamma_1) + 2A_1(\gamma_1)\rho_1(\gamma_1) + A_2(\gamma_1) - 3\rho_2^2(\gamma_1),$$

$$\phi(\gamma_1) = 6\rho_1(\gamma_1)\rho_2(\gamma_1) + 2A_1(\gamma_1)\rho_2(\gamma_1),$$

$$\Theta(\gamma_1) = \rho_1^2(\gamma_1)A_1{}'(\gamma_1) + A_2{}'(\gamma_1)\rho_1(\gamma_1) + A_3{}'(\gamma_1) - A_1{}'(\gamma_1)\rho_2^2(\gamma_1),$$

$$\Gamma(\gamma_1) = 2\rho_1(\gamma_1)\rho_2(\gamma_1)A_1'(\gamma_1) + A_2'(\gamma_1)\rho_2(\gamma_1).$$

Now at $\gamma_1 = \gamma_1^*$, substitution $\rho_1 = 0$ and $\rho_2 = \sqrt{A_2}$, into equation (9), the following is obtained:

$$\begin{aligned}
&\psi(\gamma_1^*) = -2A_2(\gamma_1^*),\\
&\phi(\gamma_1^*) = 2A_1(\gamma_1^*)\sqrt{A_2(\gamma_1^*)},\\
&\Theta(\gamma_1^*) = A_3'(\gamma_1^*) - A_1'(\gamma_1^*)A_2(\gamma_1^*),\\
&\Gamma(\gamma_1^*) = A_2'(\gamma_1^*)\sqrt{A_2(\gamma_1^*)},
\end{aligned}$$

where

$$\begin{aligned}
&A_1'(\gamma_1^*) = 0,\\
&A_2'(\gamma_1^*) = a_{13}^{[3]}w^*,\\
&A_3'(\gamma_1^*) = a_{12}^{[3]}a_{23}^{[3]}w^*.
\end{aligned}$$

Hence, condition (19) gives

$$\Theta(\gamma_1^*)\psi(\gamma_1^*) + \Gamma(\gamma_1^*)\phi(\gamma_1^*) = -2A_2(\gamma_1^*)w^*\left[a_{12}^{[3]}a_{23}^{[3]} - a_{13}^{[3]}A_1'(\gamma_1^*)\right] \neq 0.$$

That means the Hopf bifurcation has occurred at γ_1^*.

From Theorem 9, the stability condition of the stable limit cycle in $R^3_{(u,v,w)}$ is presented using the coefficient of curvature of the limit cycle [36]. For a detailed discussion, we refer to [27].

Theorem 9 The DOPZ System has a stable limit cycle in $R^3_{(u,v,w)}$, if the following conditions are true:

$$\left[\frac{3r(u_1+u^*)-r(k+k_0)}{8(a_1+w_0-u_3-w^*)kk_0}\right]\alpha_1(1-m)<\frac{3r}{4(a_1+w_0-u_3-w^*)kk_0} \tag{21}$$

Proof: - We first shift the CEP, $F_3=(u^*,v^*,w^*)$ to $(0,0,0)$ by using the following transformations $u=u_1+u^*$, $v=u_2+v^*$, $w=u_3+w^*$. Then the DOPZ system becomes:

$$\frac{du_1}{dt}=\frac{r(u_1+u^*)}{(a_1+w_0-u_3-w^*)kk_0}[-(u_1+u^*)^2+(u_1+u^*)(k+k_0)-kk_0]$$
$$-\alpha_1(u_1+u^*)(u_2+v^*)(1-m)-(u_1+u^*)\delta_1$$
$$\frac{du_2}{dt}=\frac{\alpha_2(u_1+u^*)(u_2+v^*)(1-m)}{(a_2+w_0-u_3-w^*)}-\delta_2(u_2+v^*)-a(u_1+u^*)(u_2+v^*)(1-m)$$
$$\frac{du_3}{dt}=s[w_0-(u_3+w^*)]+d(u_1+u^*)-\gamma(u_3+w^*)-\gamma_1(u_1+u^*)(u_3+w^*)$$
$$-\gamma_2(u_2+v^*)(u_3+w^*),$$

where the nonlinear part of the above system is presented in the following matrix is

$$\mho=\begin{pmatrix}\mho_1\\ \mho_2\\ \mho_3\end{pmatrix}$$
$$=\begin{pmatrix}\frac{r(u_1+u^*)}{(a_1+w_0-u_3-w^*)kk_0}[-(u_1+u^*)^2+(u_1+u^*)(k+k_0)-kk_0]-\alpha_1(1-m)u_1u_2\\ \frac{\alpha_2(u_1+u^*)(u_2+v^*)(1-m)}{(a_2+w_0-u_3-w^*)}-a(1-m)u_1u_2\\ -\gamma_1u_1u_3-\gamma_2u_2u_3\end{pmatrix}$$

We derive the following characteristic quantities from the nonlinear part:

$$g_{20}^0=\frac{1}{4}\left\{\frac{\partial^2\mho_1}{\partial u_1^2}-\frac{\partial^2\mho_1}{\partial u_2^2}+2\frac{\partial^2\mho_2}{\partial u_1\partial u_2}+i\left(\frac{\partial^2\mho_2}{\partial u_1^2}-\frac{\partial^2\mho_2}{\partial u_2^2}-2\frac{\partial^2\mho_1}{\partial u_1\partial u_2}\right)\right\}=\frac{1}{2}\left\{\frac{-3r(u_1+u^*)+r(k+k_0)}{(a_1+w_0-u_3-w^*)kk_0}+\right.$$
$$\left.\frac{\alpha_2(1-m)}{(a_2+w_0-u_3-w^*)}-a(1-m)+\alpha_1(1-m)i\right\},$$

$$g_{11}^0=\frac{1}{4}\left\{\frac{\partial^2\mho_1}{\partial u_1^2}+\frac{\partial^2\mho_1}{\partial u_2^2}+i\left(\frac{\partial^2\mho_2}{\partial u_1^2}+\frac{\partial^2\mho_2}{\partial u_2^2}\right)\right\}=\frac{1}{2}\left\{\frac{-3r(u_1+u^*)+r(k+k_0)}{(a_1+w_0-u_3-w^*)kk_0}\right\},$$

$$G_{110}^0=\frac{1}{2}\left\{\frac{\partial^2\mho_1}{\partial u_1\partial u_3}+\frac{\partial^2\mho_2}{\partial u_2\partial u_3}+i\left(\frac{\partial^2\mho_2}{\partial u_1\partial u_3}-\frac{\partial^2\mho_1}{\partial u_2\partial u_3}\right)\right\}=\frac{1}{2}\left\{\frac{-3r(u_1+u^*)^2+2r(k+k_0)}{(a_1+w_0-u_3-w^*)^2kk_0}-\frac{r}{(a_1+w_0-u_3-w^*)^2}+\right.$$
$$\left.\frac{\alpha_2(u_1+u^*)(1-m)}{(a_2+w_0-u_3-w^*)^2}+i\left(\frac{\alpha_2(u_2+v^*)(1-m)}{(a_2+w_0-u_3-w^*)^2}\right)\right\},$$

$$G_{101}^0 = \frac{1}{2}\left\{\frac{\partial^2 \upsilon_1}{\partial u_1 \partial u_3} - \frac{\partial^2 \upsilon_2}{\partial u_2 \partial u_3} + i\left(\frac{\partial^2 \upsilon_2}{\partial u_1 \partial u_3} + \frac{\partial^2 \upsilon_1}{\partial u_2 \partial u_3}\right)\right\} = \frac{1}{2}\left\{\frac{-3r(u_1+u^*)^2+2r(k+k_0)}{(a_1+w_0-u_3-w^*)^2 k k_0} - \frac{r}{(a_1+w_0-u_3-w^*)^2} - \frac{\alpha_2(u_1+u^*)(1-m)}{(a_2+w_0-u_3-w^*)^2} + i\left(\frac{\alpha_2(u_2+v^*)(1-m)}{(a_2+w_0-u_3-w^*)^2}\right)\right\},$$

$$W_{11}^0 = -\frac{1}{4\lambda_3(a_1(k^*)}\left(\frac{\partial^2 \upsilon_3}{\partial u_1^2} + \frac{\partial^2 \upsilon_3}{\partial u_2^2}\right) = 0,$$

$$W_{20}^0 = -\frac{1}{4\lambda_3(a_1(k^*)}\left(\frac{\partial^2 \upsilon_3}{\partial u_1^2} + \frac{\partial^2 \upsilon_3}{\partial u_2^2} - 2i\frac{\partial^2 \upsilon_3}{\partial u_1 \partial u_2}\right) = 0,$$

$$G_{21}^0 = \frac{1}{8}\left\{\frac{\partial^3 \upsilon_1}{\partial u_1^3} + \frac{\partial^3 \upsilon_1}{\partial u_1 \partial u_2^2} + \frac{\partial^3 \upsilon_2}{\partial u_2^3} + \frac{\partial^3 \upsilon_2}{\partial u_1^2 \partial u_2} + i\left(\frac{\partial^3 \upsilon_2}{\partial u_1^3} + \frac{\partial^3 \upsilon_2}{\partial u_1 \partial u_2^2} - \frac{\partial^3 \upsilon_1}{\partial u_2^3} - \frac{\partial^3 \upsilon_1}{\partial u_1^2 \partial u_2}\right)\right\} = \frac{-3r}{4(a_1+w_0-u_3-w^*)kk_0},$$

Thus, the coefficient of the curvature of the limit cycle of the DOPZ system (1) is given by

$$\sigma_1^0 = Re\left\{\frac{g_{20}^0 g_{11}^0}{4} i + G_{110}^0 W_{11}^0 + \frac{G_{21}^0 + G_{101}^0 W_{20}^0}{2}\right\},$$

$$\sigma_1^0 = Re\left\{\left(\frac{6r^2(u_1+u^*)^2+r^2(k+k_0)^2}{8(a_1+w_0-u_3-w^*)^2 k^2 k_0^2}\right) i + \left[\frac{3r(u_1+u^*)-r(k+k_0)}{8(a_1+w_0-u_3-w^*)kk_0}\right]\alpha_1(1-m) - \frac{3r}{4(a_1+w_0-u_3-w^*)kk_0}\right\} = \left[\frac{3r(u_1+u^*)-r(k+k_0)}{8(a_1+w_0-u_3-w^*)kk_0}\right]\alpha_1(1-m) - \frac{3r}{4(a_1+w_0-u_3-w^*)kk_0}.$$

Thus, Condition (21) guarantees that the DOPZ system has a stable limit cycle.

3.5 Numerical Simulations

To validate our theoretical conclusions and get insight into the many possible dynamics of the DOPZ model, we conduct a numerical simulation here. In this research, all figures were created in MATLAB 2019b and were constructed and designed similarly to those in references [37]–[41], and the numerical solution to our system was found using the ode45 solver. Our primary objective is to examine the dynamics of the DOPZ system when the Allee effect is amplified in phytoplankton. For the specified variables:

$$\begin{gathered}\mathrm{r} = 0.445533, k = 4, k_0 = 1, \alpha_1 = 0.4, \alpha_2 = 0.28,\ \delta_1 = 0.1, \delta_2 = 0.3, m = \\ 0.36, a_1 = 0.2, a_2 = 0.2, w_0 = 3, a = 0.1, s = 2.85, \gamma_1 = 0.18, \gamma_2 = 0.2, \gamma = \\ 0.2, d = 1,\end{gathered} \tag{22}$$

and with different initial values, it is observed from Figure 2 that $F_3 = (1.23, 2.32, 2.61)$ is a globally asymptotically stable point.

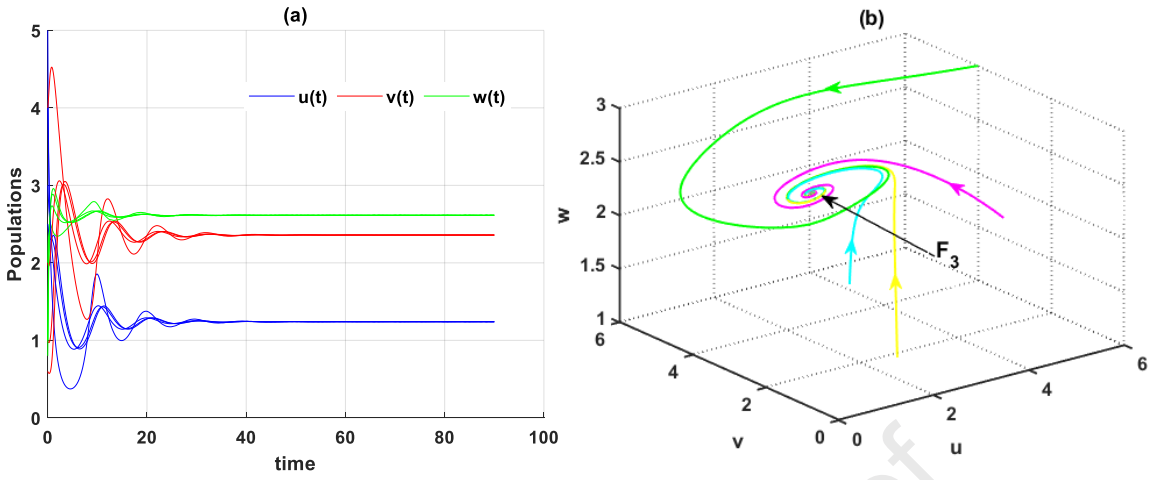

Figure 2: *Phase diagram of the DOPZ model with the data set supplied by (22) and varying initial values.*

To examine the effect of varying one parameter at a time on the behaviour of the DOPZ system, the DOPZ model has been numerically resolved for the data in (22). In light of this, Figures 3-4 investigate the effect of change in the critical phytoplankton level k_0 (Allee threshold) on the stability behaviour of the DOPZ model. The simulation shows rich dynamics when it is changed. For example, when $k_0 \leq 0.001$, the DOPZ model has no CEP, and the solution settles down to DOEP in the w- axis. While for the range $0.001 < k_0 \leq 0.01$, the solution converges asymptotically to ZFEP on uw- plane. For $0.01 < k_0 \leq 2$, the solution converges asymptotically to CEP. On the other hand, for $k_0 \geq 2.1$, the solution shows a periodic attractor behaviour.

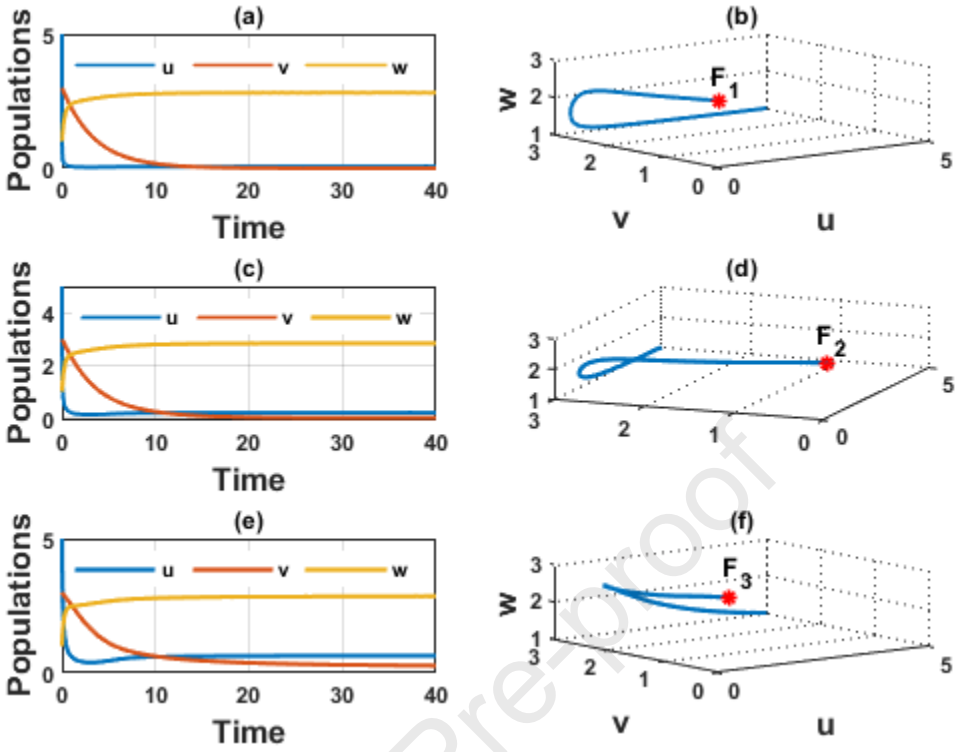

Figure 3: (a) Time series of the DOPZ system with $k_0 = 0.001$*;* ***(b)*** *phase diagram corresponding to (a);* ***(c)*** *time series with* $k_0 = 0.01$*;* ***(d)*** *phase diagram of (c);* ***(e)*** *time series with* $k_0 = 0.1$*;* ***(f)*** *phase diagram of (e).*

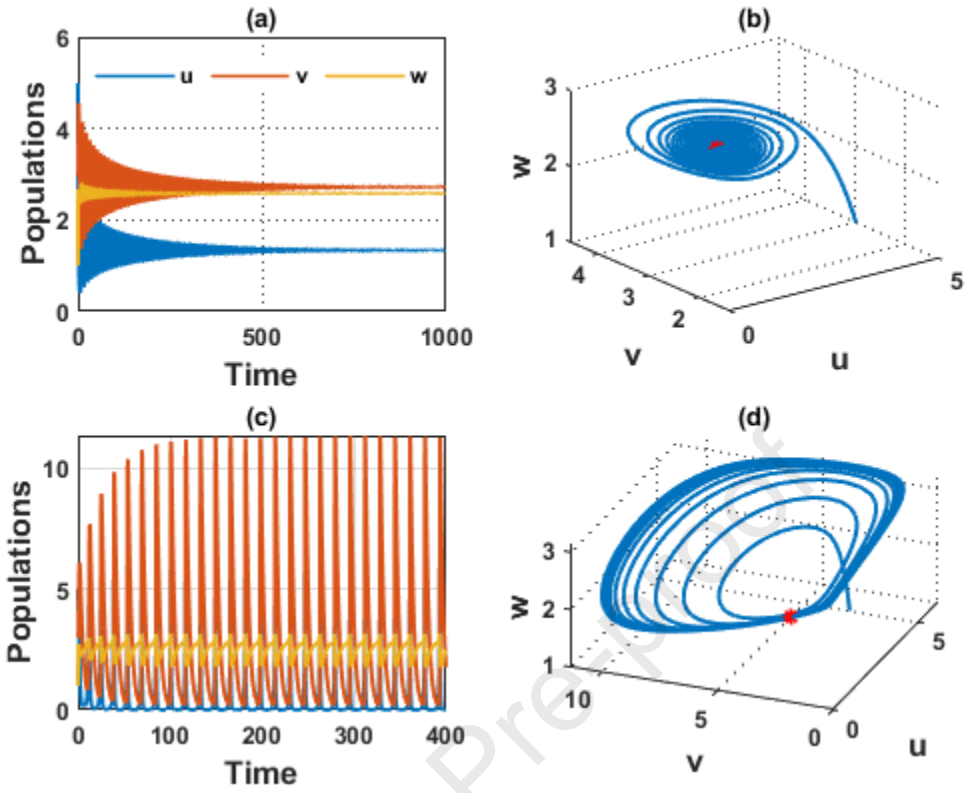

Figure 4: ***(a)*** Time series of the DOPZ system with $k_0 = 2$*;* ***(b)*** *phase diagram corresponding to (a);* ***(c)*** *time series with* $k_0 = 2.1$*;* ***(d)*** *phase diagram of (c).*

Further, Figure 5 investigates the effect of change in the consumption rate of oxygen by the phytoplankton during the night (γ_1) on the stability properties of the DOPZ model. It shows for $\gamma_1 \geq 0.78$, the DOPZ model has no CEP, and the solution settles down to ZFEP in the uw- plane. While for the range $0.001 < \gamma_1 < 0.78$, the solution converges asymptotically to CEP in an oscillatory way. On the other hand, for a small $\gamma_1 \leq 0.001$ the solution shows a periodic attractor behaviour. The latter result confirms the one that has been obtained in Theorems 8-9, which establishes the existence of Hopf bifurcation at $\gamma_1^* = 0.001$ and the stability of the obtained limit cycle.

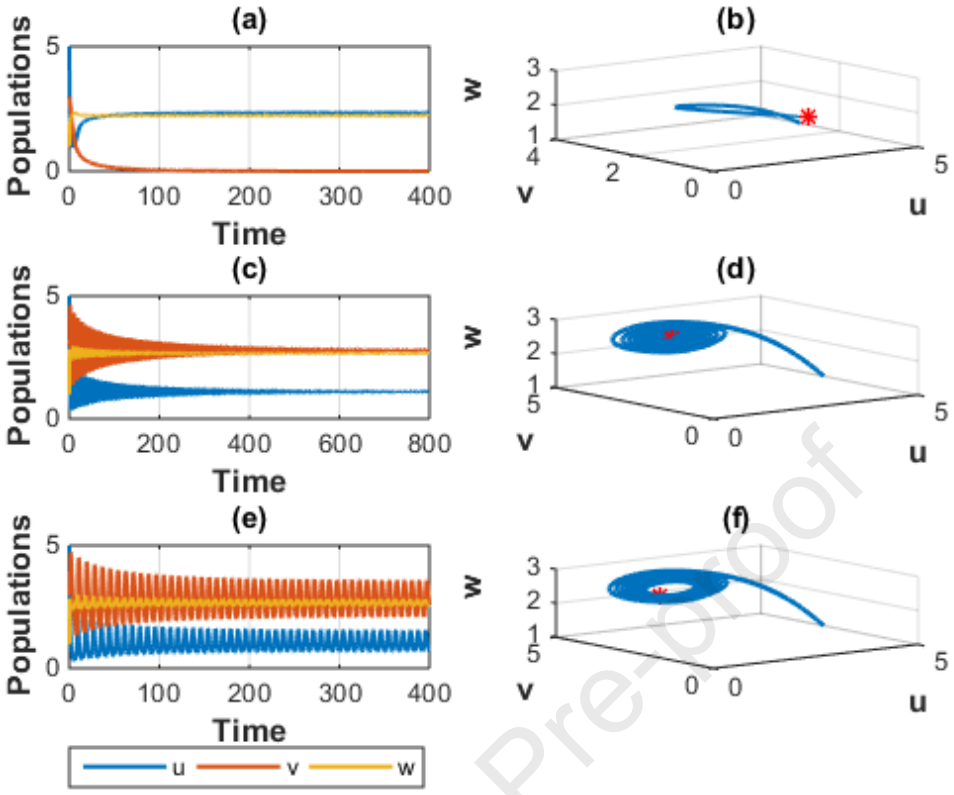

Figure 5: (a) Time series of the DOPZ system with $\gamma_1 = 0.78$*;* ***(b)*** *phase diagram corresponding to (a);* ***(c)*** *time series with* $\gamma_1 = 0.01$*;* ***(d)*** *phase diagram of (c);* ***(e)*** *time series with* $\gamma_1 = 0.001$*;* ***(f)*** *phase diagram of (e).*

Now the effect of changing the concentration of dissolved oxygen that comes from several sources (w_0) is explored in Figure 6. The figure shows that the solution settles asymptotically to the CEP, $F_3 = (0.96, 3.26, 1.77)$, for $w_0 > 1.9$. Further, the solution approaches a periodic attractor for $w_0 \leq 1.9$. Accordingly, a decrease in w_0 results in a drop in the DOPZ model's stability, which implies that condition 10 of Theorem 3 is broken and the system's (1) behavior changes from global stability to periodic behavior. The system in this instance is getting closer to a stable periodic attractor as a result of this outcome, which satisfies requirement 21 that is stated in Theorem 9.

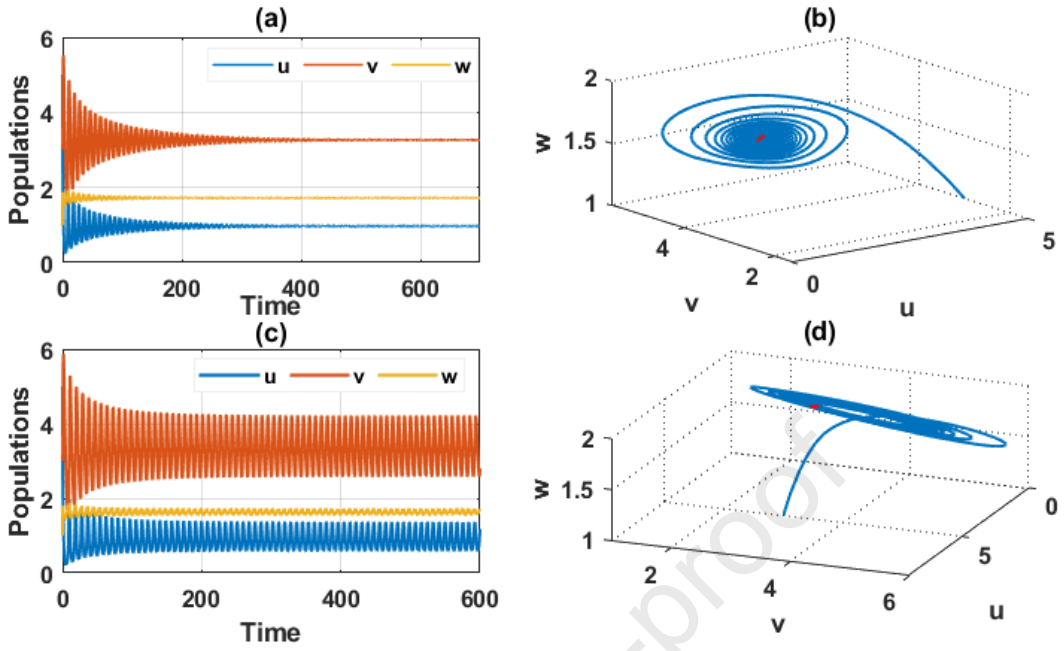

Figure 6: (a) Time series of the DOPZ system with $w_0 = 2$; ***(b)*** *phase diagram corresponding to (a);* ***(c)*** *time series with* $w_0 = 1.9$*;* ***(d)*** *phase diagram of (c).*

Further, Figure 7 illustrates the impact of varying the phytoplankton's growth rate r, on the behaviour of the DOPZ system. The solution stabilises at its positive equilibrium point CEP for $r \geq 0.1$. The solution settles down to the dissolved oxygen equilibrium point (F_1) when $r < 0.1$. Consequently, a decrease in r leads to extinction in the plankton populations hence the stability behavior shifts from the positive equilibrium point (F_3) to the dissolved oxygen equilibrium point (F_1). This result suggests that condition 21 of Theorem 9 is violated, in this case, faces a transcritical bifurcation between F_1 and F_3.

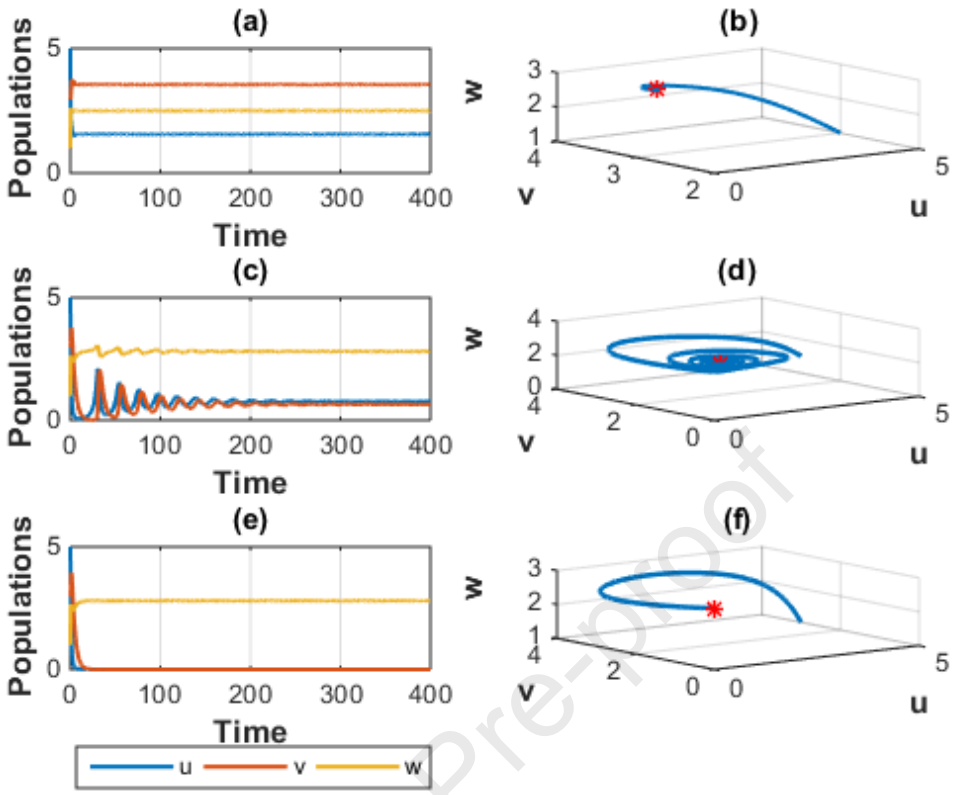

Figure 7: (a) Time series of the DOPZ system with $r = 0.9$*;* ***(b)*** *phase diagram corresponding to (a);* ***(c)*** *time series with* $r = 0.1$*;* ***(d)*** *phase diagram of (c);* ***(e)*** *time series with* $r = 0.01$*;* ***(f)*** *phase diagram of (e).*

Next, Figure 8 depicts the impact of varying the conservation rate from phytoplankton to zooplankton α_2 on the behaviour of the DOPZ system. The solution asymptotically approaches the CEP for $\alpha_2 \geq 0.1$, while the solution converges to the ZFEP in the uw- plane F_2 in Int.$R^2_{+(uw)}$ when $\alpha_2 < 0.1$. This means that F_2 loses stability at $\alpha_2 = 0.1$. As a consequence, the outcome that was given by Theorem 4 has been demonstrated to be accurate by the numerical simulations.

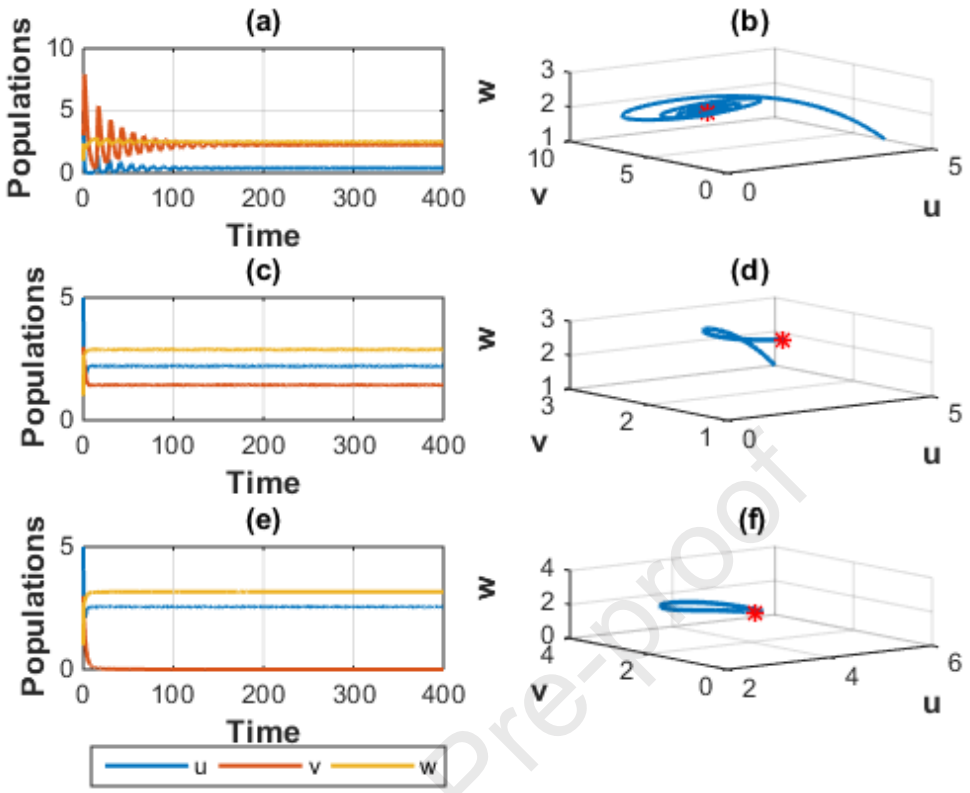

Figure 8: (a) Time series of the DOPZ system with $\alpha_2 = 0.9$*;* ***(b)*** *phase diagram corresponding to (a);* ***(c)*** *time series with* $\alpha_2 = 0.1$*;* ***(d)*** *phase diagram of (c);* ***(e)*** *time series with* $\alpha_2 = 0.01$*;* ***(f)*** *phase diagram of (e).*

In addition, Figure 9 displays the influence of varying the consumption of oxygen by zooplankton (γ_2). Clearly, the solution approaches the CEP level when $\gamma_2 \geq 0.1$. Further, for $\gamma_2 < 0.1$, the solution becomes a periodic attractor.

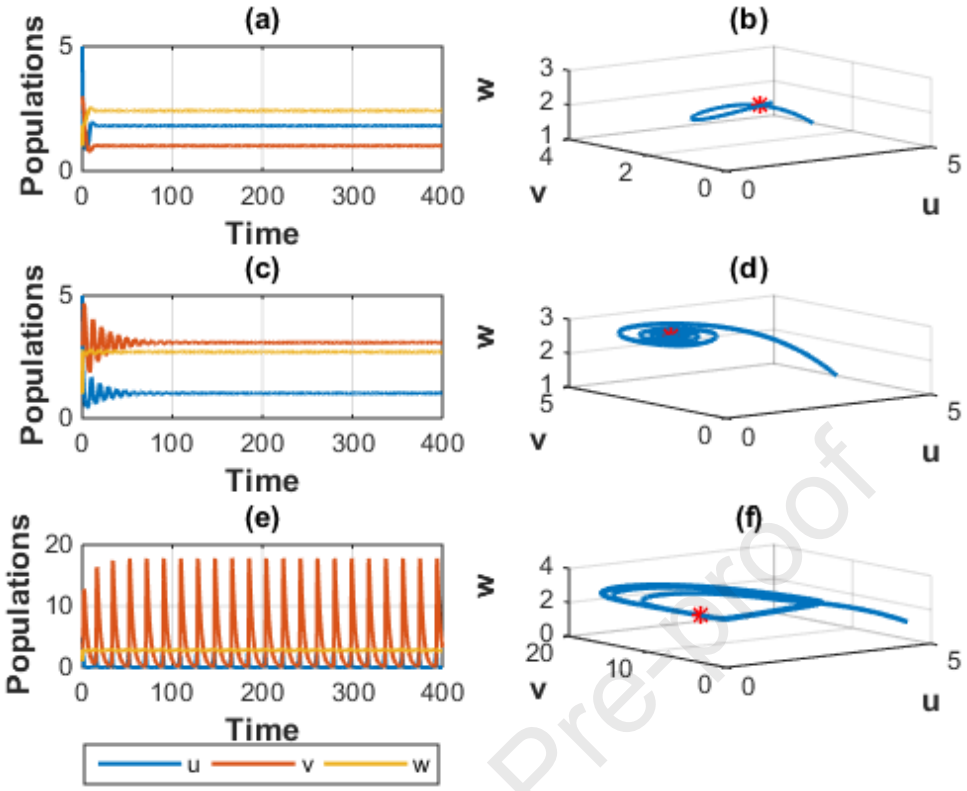

Figure 9: (a) Time series of the DOPZ system with $\gamma_2 = 0.9$*;* ***(b)*** *phase diagram corresponding to (a);* ***(c)*** *time series with* $\gamma_2 = 0.1$*;* ***(d)*** *phase diagram of (c);* ***(e)*** *time series with* $\gamma_2 = 0.01$*;* ***(f)*** *phase diagram of (e).*

Now, Figure 10 discusses the effect of changing δ_1 on the behaviour of the DOPZ. The simulation shows for $\delta_1 \leq 0.67$, the solution accesses its CEP level. Further, for $\delta_1 > 0.67$, the solution encounters a periodic attractor.

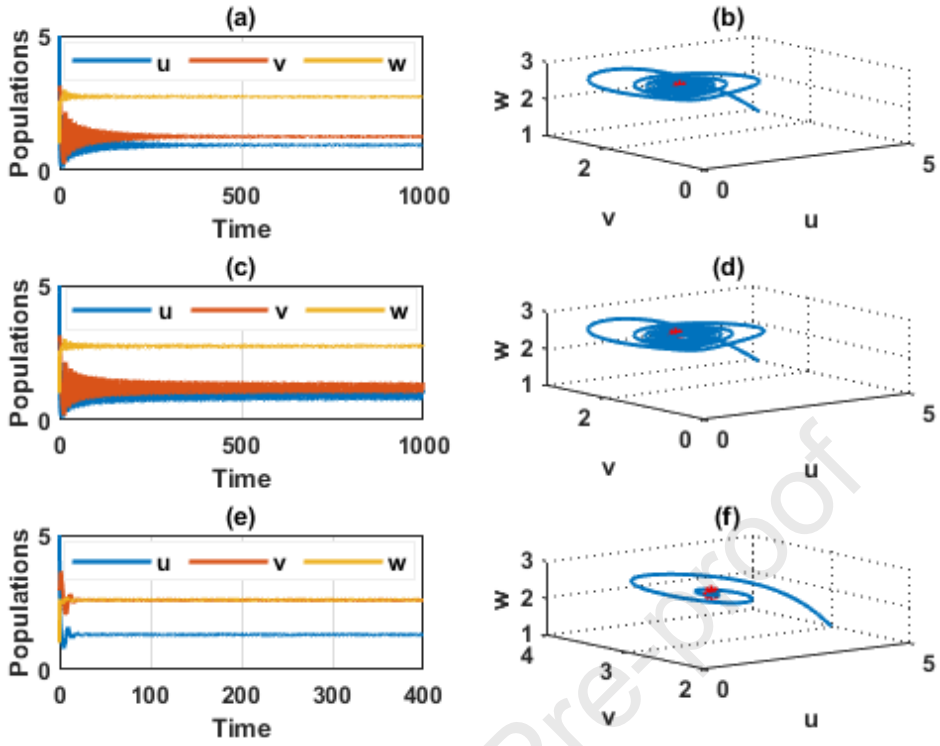

Figure 10: (a) Time series of the DOPZ system with $\delta_1 = 0.67$*;* ***(b)*** *phase diagram corresponding to (a);* ***(c)*** *time series with* $\delta_1 = 0.68$*;* ***(d)*** *phase diagram of (c);* ***(e)*** *time series with* $\delta_1 = 0.0001$*;* ***(f)*** *phase diagram of (e).*

Next, the influence of changing δ_2 is investigated in Figure 11. The simulation illustrates that for $\delta_2 \geq 0.13$, the solution stabilizes at its CEP level, while for $\delta_2 < 0.13$ the solution follows a periodic attractor.

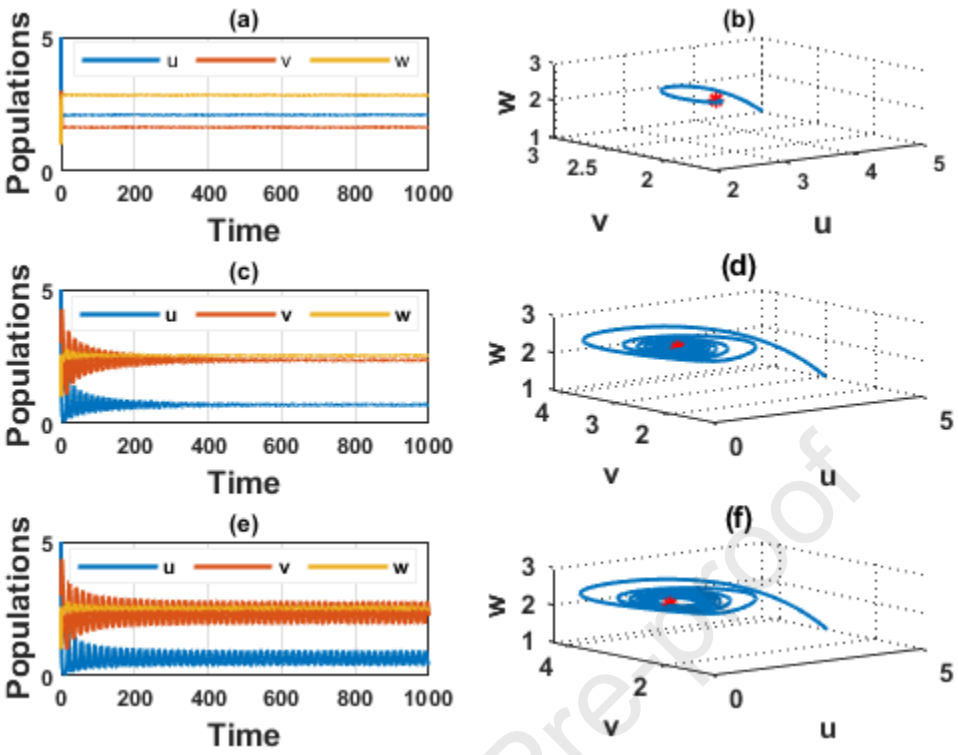

Figure 11: (a) Time series of the DOPZ system with $\delta_2 = 0.9$*;* ***(b)*** *phase diagram corresponding to (a);* ***(c)*** *time series with* $\delta_2 = 0.13$*;* ***(d)*** *phase diagram of (c);* ***(e)*** *time series with* $\delta_2 = 0.129$*;* ***(f)*** *phase diagram of (e).*

Finally, for varying the following parameters each time $\alpha_1, s, d, m, a, \gamma, a_1$ and a_2, the solution approaches its CEP in the interior of $R^3_{(u,v,w)}$. For instance, see Figures 12-19.

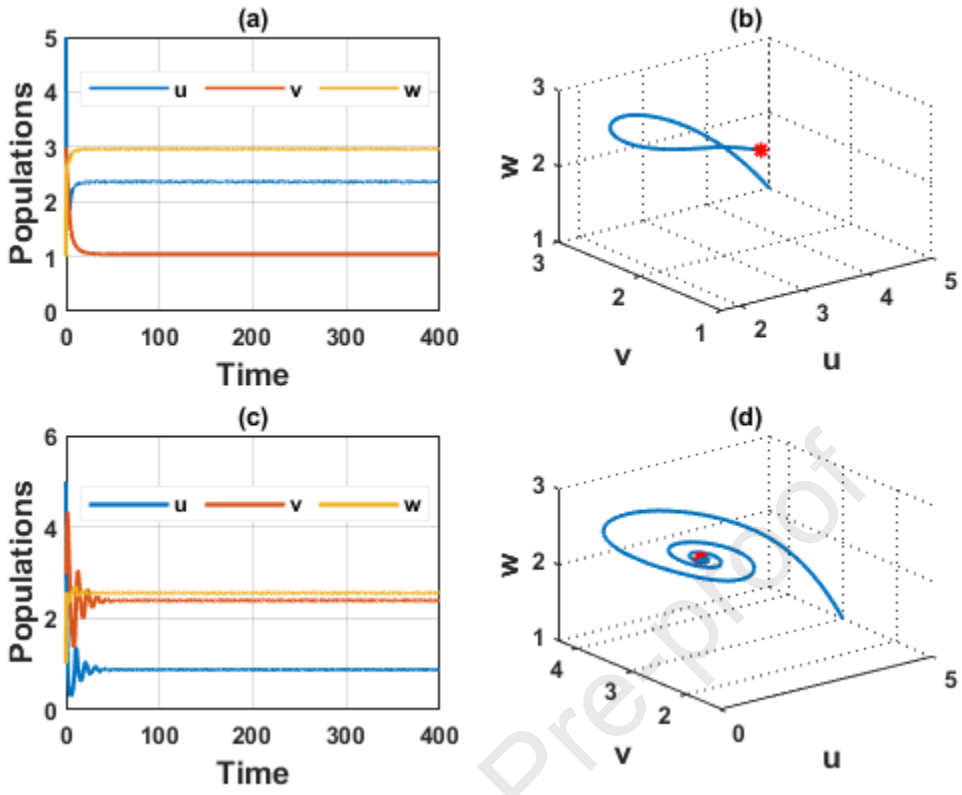

Figure 12: (a) Time series of the DOPZ system with $a_2 = 0.9$*;* ***(b)*** *phase diagram corresponding to (a);* ***(c)*** *time series with* $a_2 = 0.001$*;* ***(d)*** *phase diagram of (c).*

4. Discussion

This paper modified the dissolved oxygen-plankton model to include a strong Allee effect in the phytoplankton population taking into account that the zooplankton feeds on both toxic and non-toxic phytoplankton. The idea is to figure out how this kind of growth affects the dynamics of an aquatic environment. The system underwent theoretical and numerical analysis. The theoretical results detect that there are three steady states; the first one is the dissolved oxygen equilibrium point DOEP which always has stable behaviour. The second one is the zooplankton-free equilibrium point ZFEP which shows stable behaviour under certain conditions; otherwise, it could have become unstable, leading to bifurcations of saddle-node or periodic nature. The third one is CEP which also could be stable or unstable depending on specific conditions. The essential conditions have been found to ensure the happening of different types of bifurcation around the ZFEP and CEP. Nonetheless, the numerical simulation deduced when the stability criteria are met, the DOPZ system always sways about the CEP. Further, changing the critical phytoplankton level k_0 (Allee threshold), the solution presents diverse dynamics, such as extinction only for the phytoplankton population, extinction for both plankton species, persistence of all components, or periodic attractor dynamics. Thus, it can be considered a critical parameter affecting the whole system's dynamics. Moreover, for large γ_1, the consumption rate of oxygen by the phytoplankton

during the night, and for small α_2, the zooplankton population undergoes extinction, and so the solution of the DOPZ system is moved from the CEP to a ZFEP. In addition, for small r, the phytoplankton's growth rate, both phytoplankton and zooplankton populations face extinction. However, for small γ_1, γ_2, δ_2 w_0, the DOPZ system shows limit cycle behaviour. The same behaviour could be detected for large δ_1. Finally, the solution is stabilized at the CEP when the remaining parameters are changed.

5. **Conclusion**

The strong Allee effect type of growth term for the phytoplankton population was incorporated in this work. This seems necessary since phytoplankton, which is responsible for an estimated 50-80% of the world's oxygen generation, is becoming more and more endangered because of the increase in waste thrown into the water, in particular industrial waste. This, in turn, leads to damage of the other marine species. Therefore, it is reasonable to ask: How could we avoid the extinction of phytoplankton? Theorem 3 shows the conditions which guarantee that phytoplankton and zooplankton populations can coexist in a stable state. However, the simulation shows the system demonstrates many phenomena such as coexistence, extinction, and the limit cycle by altering the parametric values. These phenomena are fundamental characteristics of non-linear models. Further, the simulation illustrations that if k_0 (Allee threshold of the phytoplankton population) and γ (The natural depletion rate of oxygen) cannot be controlled, the two species are threatened with extinction. For instance, the plankton population faces extinction at $k_0 \leq 0.001$, while zooplankton faces extinction for $0.001 < k_0 \leq 0.01$. For $0.01 < k_0 \leq 2$, the solution stabilized at the coexistence state. However, when $k_0 \geq 2.1$, the solution exhibits periodic attractor behavior.

Finally, we suggest considering a stage structure for the zooplankton population in future work by expanding the model to include a system with four components. Further, the zooplankton population are assumed to grow logistically in the absence of the phytoplankton species, in this case, the latter is considered additional food for zooplankton.

Declarations

Competing interests: The authors declare no conflict of interest.

Authors' contributions: Conceptualization; AA & SJ. Writing - original draft preparation; AA & SJ. Methodology; SJ & AHA. Software; AHA. Visualization; AHA. Formal analysis and investigation; AA & SJ & MW. Writing - review and editing: AHA & MW. Resources; AA. Supervision: MW.

Availability of data and materials: Data sharing is not applicable to this article as no data-sets were generated or analyzed during this study.

APPENDIX

The coefficient of equation (2) is defined below as:

$$B_0 = a^2(am_1 - \gamma_1 m_2),$$

$$B_1 = 3a^2 m_1 m_3 + a^2\gamma_1 m_2 m_4 + a^2 m_2 m_7(d + \gamma_1) - a^3 m_5 - a^3 m_1 m_4 - 2am_2 m_6$$

$$\begin{aligned} B_2 = {} & m_1[2\alpha_2^2 a - 4\alpha_2 a^2 a_2 - 4\alpha_2 a^2 w_0 + 3a^2 a_2^2 + 6a^3 a_2 w_0 + 2a^3 w_0^2 + \alpha_2 a - 2\alpha_2 a^2 a_2 \\ & - 2\alpha_2 a^2 w_0 + a^3 w_0^2] - 3a^2 m_5 m_3 + a^3 m_4 m_5 - 3a^2 m_1 m_3 m_4 \\ & + m_2[2\gamma_1 m_6 m_4 - (\alpha_2 - 2\alpha_2 a m_7 + a^2 a_2^2 + 2a^2 a_2 w_0 + a^2 w_0) - a^2 m_4 \\ & + 2m_6 m_7(d + \gamma) - a^2 d m_7] + \gamma_1 r\delta^2 + a(m_8 - m_9) \end{aligned}$$

$$\begin{aligned} B_3 = {} & m_1[\alpha_2^3 - 3\alpha_2^2 a a_2 - 3\alpha_2^2 a w_0 + 3\alpha_2 a^2 a_2^2 + 6\alpha_2 a^2 a_2 w_0 + 4\alpha_2 a^2 w_0^2 - a^3 a_2^3 - 3a^3 a_2^3 w_0 \\ & - a^2 a_2 w_0^2 - 2a^3 a_2 w_0^2 + a^3 w_0^3] \\ & - m_5[2\alpha_2^2 a - 4\alpha_2 a^2 a_2 - 4\alpha_2 a^2 w_0 + 3a^2 a_2^2 + 6a^3 a_2 w_0 + 2a^3 w_0^2 + \alpha_2 a \\ & - 2\alpha_2 a^2 a_2 - 2\alpha_2 a^2 w_0 + a^3 w_0^2] + 3a^2 m_5 m_4 \\ & - m_1 m_4[2\alpha_2^2 a - 4\alpha_2 a^2 a_2 - 4\alpha_2 a^2 w_0 + 3a^3 a_2^2 + 4a^3 a_2 w_0 + 2a^3 w_0^2 + \alpha_2 a \\ & - 2\alpha_2 a^2 a_2 - \alpha_2 a^2 w_0 + 2a^3 a_2 w_0 + a^3 w_0] + m_2[\gamma_1 m_4(\alpha_2 - 2\alpha_2 a a_2 \\ & - 2\alpha_2 a w_0 + a^2 a_2^2 + 2a^2 a_2 w_0 + a^2 w_0) - 2am_3 m_4 - (\alpha_2 - 2\alpha_2 a a_2 - 2\alpha_2 a w_0 \\ & + a^2 a_2^2 + 2a^2 a_2 w_0 + a^2 w_0)(d + \gamma_1)m_7 + (a^2 m_4 - 2am_3)(dm_7)] \\ & - 2\gamma_1 r\delta^2 m_7 - m_8(2am_7 - \alpha_2) + m_9(ra + \delta_1 a m_4 - \alpha_2 + am_7)B_4 \\ & = m_4 m_5[2\alpha_2^2 a - 4\alpha_2 a^2 a_2 - 4\alpha_2 a^2 w_0 + 3a^2 a_2^2 + 6a^3 a_2 w_0 + 2a^3 w_0^2 + \alpha_2 a \\ & - 2\alpha_2 a^2 a_2 - 2\alpha_2 a^2 w_0 + 3a^3 w_0^2] \\ & - m_5[\alpha_2^3 - 3\alpha_2^2 a a_2 - 3\alpha_2^2 a w_0 + 3\alpha_2 a^2 a_2^2 + 6\alpha_2 a^2 a_2 w_0 + 4\alpha_2 a^2 w_0^2 - a^3 a_2^3 \\ & - 3a^3 a_2^3 w_0 - a^2 a_2 w_0^2 - 2a^3 a_2 w_0^2 + a^3 w_0^3] \\ & - m_1 m_4[\alpha_2^3 - 3\alpha_2^2 a a_2 - 3\alpha_2^2 a w_0 + 3\alpha_2 a^2 a_2^2 + 6\alpha_2 a^2 a_2 w_0 + 4\alpha_2 a^2 w_0^2 \\ & - a^3 a_2^3 - 3a^3 a_2^3 w_0 - a^2 a_2 w_0^2 - 2a^3 a_2 w_0^2 + a^3 w_0^3] \\ & + m_2[2am_3 m_4 - dm_7(\alpha_2 - 2\alpha_2 a a_2 - 2\alpha_2 a w_0 + a^2 a_2^2 + 2a^2 a_2 w_0 + a^2 w_0) \\ & - (\alpha_2 - 2\alpha_2 a a_2 - 2\alpha_2 a w_0 + a^2 a_2^2 + 2a^2 a_2 w_0 + a^2 w_0^2)(dm_4 + \gamma_1 m_4 m_7)] \\ & + \gamma_1 r\delta_1^2 m_7^2 - m_7(\alpha_2 m_8 + am_7) + m_9(r\alpha_2 - ram_7 + \delta_1 \alpha_2 m_4 - a\delta_1 m_4 m_7) \end{aligned}$$

$$\begin{aligned} B_5 = {} & m_4 m_5[\alpha_2^3 - 3\alpha_2^2 a a_2 - 3\alpha_2^2 a w_0 + 3\alpha_2 a^2 a_2^2 + 6\alpha_2 a^2 a_2 w_0 + 4\alpha_2 a^2 w_0 - a^3 a_2^3 \\ & - 3a^3 a_2^3 w_0 - a^2 a_2 w_0^2 - 2a^3 a_2 w_0^2 + a^3 w_0^3] \\ & + m_2 m_4 m_7 d(\alpha_2 - 2\alpha_2 a a_2 - 2\alpha_2 a w_0 + a^2 a_2^2 + 2a^2 a_2 w_0 + a^2 w_0^2). \end{aligned}$$

Here $m_1 = (s + \gamma)(1 - m)^4 \alpha_1 k k_0$, $m_2 = \delta_1 \alpha_1 k k_0 (1 - m)^3$, $m_3 = \alpha_2 - a a_2 - a w_0$, $m_4 = a_1 + w_0$, $m_5 = s w_0 \alpha_1 k k_0 (1 - m)^4$, $m_6 = \alpha_2 a - a a_2^2 - a^2 w_0$, $m_7 = a_2 + w_0$, $m_8 = r\gamma_1 \delta_1 (k + k_0)(1 - m)$, $m_9 = \gamma_1 k k_0 (1 - m)$.

References

[1] V. Hull, L. Parrella, and M. Falcucci, "Modelling dissolved oxygen dynamics in coastal lagoons," *Ecol. Modell.*, vol. 211, no. 3–4, pp. 468–480, 2008.

[2] A. K. Misra, "Modeling the depletion of dissolved oxygen in a lake due to submerged macrophytes," *Nonlinear Anal. Model. Control*, vol. 15, no. 2, pp. 185–198, 2010.

[3] A. K. Misra, P. Chandra, and V. Raghavendra, "Modeling the depletion of dissolved oxygen in a lake due to algal bloom: Effect of time delay," *Adv. Water Resour.*, vol. 34, no. 10, pp. 1232–1238, 2011.

[4] Y. Sekerci and S. Petrovskii, "Mathematical modelling of plankton–oxygen dynamics under the climate change," *Bull. Math. Biol.*, vol. 77, no. 12, pp. 2325–2353, 2015.

[5] K. Hancke and R. N. Glud, "Temperature effects on respiration and photosynthesis in three diatom-dominated benthic communities," *Aquat. Microb. Ecol.*, vol. 37, no. 3, pp. 265–281, 2004.

[6] S. Mandal, S. Ray, and P. B. Ghosh, "Modeling nutrient (dissolved inorganic nitrogen) and plankton dynamics at Sagar island of Hooghly–Matla estuarine system, West Bengal, India," *Nat. Resour. Model.*, vol. 25, no. 4, pp. 629–652, 2012.

[7] A. Gökçe, "A mathematical study for chaotic dynamics of dissolved oxygen-phytoplankton interactions under environmental driving factors and time lag," *Chaos, Solitons & Fractals*, vol. 151, p. 111268, 2021.

[8] H. Hao, R. Mo, S. Kang, and Z. Wu, "Effects of temperature, inlet gas pressure and humidity on PEM water contents and current density distribution," *Results Eng.*, vol. 20, p. 101411, 2023.

[9] S. Mondal, G. Samanta, and M. De la Sen, "Dynamics of Oxygen-Plankton Model with Variable Zooplankton Search Rate in Deterministic and Fluctuating Environments," *Mathematics*, vol. 10, no. 10, p. 1641, 2022.

[10] S. M. Salman and A. A. Elsadany, "Higher order codimension bifurcations in a discrete-time toxic-phytoplankton–zooplankton model with Allee effect," *Int. J. Nonlinear Sci. Numer. Simul.*, 2022.

[11] M. S. Surendar and M. Sambath, "Qualitative Analysis for a Phytoplankton-Zooplankton Model with Allee Effect and Holling Type II Response," *Discontinuity, Nonlinearity, Complex.*, vol. 10, no. 01, pp. 1–18, 2021.

[12] Q. Lin, "Allee effect increasing the final density of the species subject to the Allee effect in a Lotka–Volterra commensal symbiosis model," *Adv. Differ. Equations*, vol. 2018, no. 1, pp. 1–9, 2018.

[13] X. Pan, M. Zhao, Y. Wang, H. Yu, Z. Ma, and Q. Wang, "Stability and dynamical analysis of a biological system," in *Abstract and Applied Analysis*, 2014, vol. 2014.

[14] S. R. Jawad and M. Al Nuaimi, "Persistence and bifurcation analysis among four species interactions with the influence of competition, predation and harvesting," *Iraqi J. Sci.*, pp. 1369–1390, 2023.

[15] S. Dawud and S. Jawad, "Stability analysis of a competitive ecological system in a polluted environment," *Commun. Math. Biol. Neurosci.*, vol. 2022, p. Article-ID, 2022.

[16] M. Al Nuaimi and S. Jawad, "Modelling and stability analysis of the competitional ecological model with harvesting," *Commun. Math. Biol. Neurosci.*, vol. 2022, p. Article-ID, 2022.

[17] Sajan, S. K. Sasmal, and B. Dubey, "A phytoplankton–zooplankton–fish model with chaos control: In the presence of fear effect and an additional food," *Chaos An Interdiscip. J. Nonlinear Sci.*, vol. 32, no. 1, p. 13114, 2022.

[18] A. Vodeniktov, V. Melnikova, A. Minibaev, and N. Lazarev, "Control of condensate dissolved oxygen in steam surface condenser. Reconstruction experience," *Results Eng.*, vol. 15, p. 100492, 2022.

[19] X.-Y. Meng and L. Xiao, "Stability and Bifurcation for a Delayed Diffusive Two-Zooplankton One-Phytoplankton Model with Two Different Functions," *Complexity*, vol. 2021, 2021.

[20] T. G. Hallam, C. E. Clark, and G. S. Jordan, "Effects of toxicants on populations: a qualitative approach II. First order kinetics," *J. Math. Biol.*, vol. 18, no. 1, pp. 25–37, 1983.

[21] S. Chakraborty, S. Chatterjee, E. Venturino, and J. Chattopadhyay, "Recurring plankton bloom dynamics modeled via toxin-producing phytoplankton," *J. Biol. Phys.*, vol. 33, no. 4, pp. 271–290, 2007.

[22] J. Dhar and R. S. Baghel, "Role of dissolved oxygen on the plankton dynamics in spatio-temporal domain," *Model. Earth Syst. Environ.*, vol. 2, no. 1, pp. 1–15, 2016.

[23] V. P. Dubey, J. Singh, A. M. Alshehri, S. Dubey, and D. Kumar, "Numerical investigation of fractional model of phytoplankton–toxic phytoplankton–zooplankton system with convergence analysis," *Int. J. Biomath.*, vol. 15, no. 04, p. 2250006, 2022.

[24] L. Niu, Q. Chen, and Z. Teng, "Bifurcation analysis in a discrete toxin-producing phytoplankton–zooplankton model with refuge," *J. Differ. Equations Appl.*, pp. 1–26, 2024.

[25] R. Chandra, P. Gupta, and A. Priyadarshi, "Holling type-II functional response in aquatic ecosystem models shaping spatial heterogeneous distribution of Phytoplankton data at Tokyo Bay," in *AIP Conference Proceedings*, 2024, vol. 3087, no. 1.

[26] W. Zhang, S. Han, D. Zhang, B. Shan, and D. Wei, "Variations in dissolved oxygen and aquatic biological responses in China's coastal seas," *Environ. Res.*, vol. 223, p. 115418, 2023.

[27] M. W. Hirsch, S. Smale, and R. L. Devaney, *Differential equations, dynamical systems, and an introduction to chaos*. Academic press, 2012.

[28] P. Hartman, “Ordinary Differential Equations 2nd edn (Philadelphia, PA: SIAM),” 2002.

[29] A. K. Paul, N. Basak, and M. A. Kuddus, “Mathematical analysis and simulation of COVID-19 model with booster dose vaccination strategy in Bangladesh,” *Results Eng.*, vol. 21, p. 101741, 2024.

[30] J. H. Hubbard and B. H. West, *Differential equations: A dynamical systems approach: Ordinary differential equations*, vol. 5. Springer, 2013.

[31] L. Perko, *Differential equations and dynamical systems*, vol. 7. Springer Science & Business Media, 2013.

[32] J. P. LaSalle, “Stability theory and invariance principles,” in *Dynamical systems*, Elsevier, 1976, pp. 211–222.

[33] R. M. May, *Stability and complexity in model ecosystems*. Princeton university press, 2019.

[34] Z. U. Rehman, Z. Hussain, Z. Li, T. Abbas, and I. Tlili, “Bifurcation analysis and multi-stability of chirped form optical solitons with phase portrait,” *Results Eng.*, p. 101861, 2024.

[35] Y. A. Kuznetsov, *Elements of applied bifurcation theory*, vol. 112. Springer Science & Business Media, 2013.

[36] D. Mukherjee, “Study of fear mechanism in predator-prey system in the presence of competitor for the prey,” *Ecol. Genet. Genomics*, vol. 15, p. 100052, 2020.

[37] A. A. Yinusa, M. G. Sobamowo, and A. O. Adelaja, “Thermal analysis of nanofluidic flow through multi-walled carbon nanotubes subjected to perfectly and imperfectly bonded wall conditions,” *Chem. Thermodyn. Therm. Anal.*, vol. 5, p. 100028, 2022.

[38] M. Al-Raeei, “Morse potential specific bond volume: A simple formula with applications to dimers and soft–hard slab slider,” *J. Phys. Condens. Matter*, vol. 34, no. 28, p. 284001, 2022.

[39] M. A. E. Abdelrahman and A. Alharbi, “Analytical and numerical investigations of the modified Camassa–Holm equation,” *Pramana*, vol. 95, pp. 1–9, 2021.

[40] A. A. Thirthar, P. Panja, A. Khan, and M. A. Alqudah, “An Ecosystem Model with Memory Effect Considering Global Warming,” *J. Theor. Biol*, vol. 419, pp. 13–22, 2017.

[41] S. K. Hassan and S. R. Jawad, “The Effect of Mutual Interaction and Harvesting on Food Chain Model,” *Iraqi J. Sci.*, pp. 2641–2649, 2022.

The highlights of our paper are:

1- A depletion dissolved oxygen-plankton model is considered for an aquatic environment.
2- Phytoplankton population is subjected to a strong Allee effect.
3- Derived the condition of stability in the aquatic system.
4- Transcritical and Hopf bifurcation behavior of the proposed system is observed.

Declaration of interests

☒ The authors declare that they have no known competing financial interests or personal relationships that could have appeared to influence the work reported in this paper.

☐ The authors declare the following financial interests/personal relationships which may be considered as potential competing interests: